Calcium tunneling through the ER and transfer to other organelles for optimal signaling in *Toxoplasma gondii*.

Zhu-Hong Li[1], Beejan Asady[1,2], Le Chang[1], Miryam Andrea Hortua Triana[1], Catherine Li[1], Isabelle Coppens[2] and Silvia N.J. Moreno[1,3*]

[1]Center for Tropical and Emerging Global Diseases, Department of Computes Science, University of Georgia and [3]Department of Cellular Biology, University of Georgia, Athens, Georgia 30602

[2]Department of Molecular Microbiology and Immunology, Johns Hopkins Bloomberg School of Public Heath, Baltimore, MD 21205

Running title: Intracellular Ca^{2+} stores of *T. gondii*

[*]To whom correspondence should be addressed: Silvia N. J. Moreno, Department of Cellular Biology and Center for Tropical and Emerging Global Disease, 350A Paul D. Coverdell Center, University of Georgia, Athens, GA 30602. Tel.: 706-542-4736; Fax: 706-542-9493; E-mail: smoreno@uga.edu

Keywords: Calcium, endoplasmic reticulum, membrane contact sites, Toxoplasma gondii, SERCA-Ca^{2+}-ATPase, calcium tunneling

ABSTRACT

Ca^{2+} signaling in cells begins with the opening of Ca^{2+} channels in either the plasma membrane (PM) or the endoplasmic reticulum (ER) and results in a dramatic increase in the physiologically low (<100 nM) cytosolic Ca^{2+} level. The temporal and spatial Ca^{2+} levels are well regulated to enable precise and specific activation of critical biological processes. Ca^{2+} signaling regulates pathogenic features of apicomplexan parasites like *Toxoplasma gondii* which infects approximately one-third of the world's population. *T. gondii* relies on Ca^{2+} signals to stimulate traits of its infection cycle and several Ca^{2+} signaling elements play essential roles in its parasitic cycle. Active egress, an essential step for the infection cycle of *T. gondii* is preceded by a large increase in cytosolic Ca^{2+} most likely by release from intracellular stores. Intracellular parasites take up Ca^{2+} from the host cell during host Ca^{2+} signaling events to replenish intracellular stores. In this work, we investigated the mechanism by which intracellular stores are replenished with Ca^{2+} and demonstrated a central role for the SERCA-Ca^{2+}-ATPase to keep not only the ER filled with Ca^{2+} but also acidic stores. We also show mitochondrial Ca^{2+} uptake, by transfer of Ca^{2+} from the ER most likely through membrane contact sites. We propose a central role for the ER in tunneling of calcium from the extracellular milieu through the ER to other organelles.

HIGHLIGHTS

- The *T. gondii* ER efficiently takes up Ca^{2+} that enters the cytosol from the extracellular milieu.
- Filling of acidic stores in *T. gondii* appears to be dependent on the filling of the ER
- The mitochondrion of *T. gondii* has no direct access to extracellular calcium but is able to take up Ca^{2+} by transfer from the ER and/or acidic stores

INTRODUCTION

Toxoplasma gondii is an intracellular parasite from the Apicomplexan Phylum that infects approximately one third of the world population (Weiss and Dubey, 2009). During the initial infection with *T. gondii*, the parasite engages in multiple rounds of a lytic cycle, which consists of invasion of host cells, replication inside a parasitophorous vacuole (PV), exit from the host cell causing its lysis followed by invasion of a new host cell (Black and Boothroyd, 2000; Blader *et al.*, 2015). Cytosolic Ca^{2+} ($[Ca^{2+}]_c$) fluctuations precede the activation of several key steps of the *T. gondii* lytic cycle like motility, attachment, invasion, and egress ($[Ca^{2+}]_c$) (Lourido and Moreno, 2015; Hortua Triana *et al.*, 2018). Egress from the host cell is an essential step for the infection cycle of *T. gondii* (Bisio and Soldati-Favre, 2019) and it was shown that it is preceded by a cytosolic Ca^{2+} increase (Endo *et al.*, 1982; Borges-Pereira *et al.*, 2015). Extracellular Ca^{2+} entry was demonstrated in extracellular (Pace *et al.*, 2014; Hortua Triana *et al.*, 2024) and intracellular replicating tachyzoites (Vella *et al.*, 2021). This activity was highly regulated and recent work from our lab showed that a TRP-like activity was involved (Marquez-Nogueras *et al.*, 2021).

Ca^{2+} signaling is part of the signaling pathways that regulate a large number of cellular functions (Clapham, 2007). All cells express a variety of channels, transporters, and Ca^{2+} pumps, located at the plasma membrane (PM) and/or intracellular organelles (endoplasmic reticulum (ER), acidic stores, and mitochondria) that regulate/control the concentration of cytosolic Ca^{2+} ($[Ca^{2+}]_c$). A high cytosolic Ca^{2+} concentration for sustained lengths of time, is toxic to cells and may result in their death (Bootman and Bultynck, 2020).

In *T. gondii*, both Ca^{2+} entry through the plasma membrane and influx from intracellular stores like the ER may initiate a cascade of signaling events important for the stimulation of the biological steps of the parasite lytic cycle (Lourido and Moreno, 2015; Hortua Triana *et al.*, 2018). Ca^{2+} oscillations were observed in motile parasites loaded with fluorescent Ca^{2+} indicators, (Lovett and Sibley, 2003) as well as expressing Genetically Encoded Calcium Indicators (GECIs) (Borges-Pereira *et al.*, 2015). The significance of Ca^{2+} signals during all stages of the lytic cycle has been demonstrated, but little is known about the mechanism by which intracellular stores contribute to cytosolic Ca^{2+} signals and downstream regulation.

The ER, an exclusive organellar feature of eukaryotic cells, is the main store for Ca^{2+} in most eukaryotic cells and it is widely accepted that: the ER is functionally heterogeneous with Ca^{2+} binding proteins and Ca^{2+} pumps and channels having a nonuniform distribution resulting in the presence of distinct subdomains within the organelle (Papp *et al.*, 2003); the ER facilitates Ca^{2+} tunneling through its lumen as a mechanism of delivering Ca^{2+} to targeted sites without activating inappropriate processes in the cell cytosol (Petersen *et al.*, 2017); and the ER is ubiquitously distributed and is in close contact with all cellular organelles and the plasma membrane (PM) (Spang, 2018). Over the past decade a new paradigm has emerged that seeks to decipher how subcellular organelles communicate with each other in order to coordinate activities and efficiently distribute ions and lipids within the cell. Numerous observations have highlighted the presence of tight, stable and yet non-fusogenic associations between organellar membranes which have since become known as membrane contact sites (MCSs) (Phillips and Voeltz, 2016).

The secretory pathway of *T. gondii* is organized in a highly polarized manner with the ER being an extension of the nuclear envelope (Hager *et al.*, 1999; Tomavo *et al.*, 2013). The ER at the apical surface of the nuclear envelope continues with the Golgi stacks and then the secretory organelles, micronemes and rhoptries, which are unique to the apicomplexan phylum (Hager *et al.*, 1999). These organelles perform important functions relevant to a successful lytic cycle like host cell attachment, invasion, and establishment of the parasitophorous vacuole (PV). Cytoplasmic Ca^{2+} increases, due to efflux from the ER, have been reported to initiate responses like microneme secretion (Carruthers and Sibley, 1999; Nagamune *et al.*, 2007b), conoid extrusion (Del Carmen *et al.*, 2009), invasion (Vieira and Moreno, 2000; Lovett and Sibley, 2003) and egress (Arrizabalaga and Boothroyd, 2004). These responses require precise spatiotemporal control of diverse targets and suggests the presence of distinct systems to deliver Ca^{2+} to specific locations rather than allowing global increases, which would activate unnecessary and potentially detrimental signaling events (Huet and Moreno, 2023).

In order to concentrate Ca^{2+} ions, the ER utilizes a SERCA-Ca^{2+}-ATPase, a transmembrane P-type ATPase, that couples ATP hydrolysis to the transport of ions across biological membranes and against a concentration gradient. SERCA pumps can be inhibited by various inhibitors including the very potent and highly specific thapsigargin (TG) (Thastrup *et al.*, 1990; Sagara and Inesi, 1991).

T. gondii expresses a SERCA Ca^{2+}-ATPase (TgSERCA), which possess SERCA conserved domains and Ca^{2+} binding sites and ATPase residues (Nagamune *et al.*, 2007a). The function of TgSERCA was determined by rescue experiments of yeast cells defective in Ca^{2+}-ATPases and by its specific inhibition by TG (Nagamune *et al.*, 2007a). TgSERCA was mainly localized to the ER of *T. gondii* but also showed a distinct distribution in extracellular parasites, where the protein was partially found in ER vesicles in the apical region near micronemes (Nagamune *et al.*, 2007a). This distribution pattern was different to the one obtained with the transient transfection of GFP-HDEL (an ER marker), which was retained near the nuclear envelope, suggesting an uneven distribution of ER markers in extracellular parasites. The authors suggested that this distribution to the apical end may be important for rapid release and effective recovery of cytosolic Ca^{2+}, events that likely govern both motility and microneme secretion (Nagamune *et al.*, 2007a; Nagamune *et al.*, 2007b).

In this work we characterize the mechanism by which the ER efficiently takes up Ca^{2+} promptly after the ion enters the cytosol from the extracellular milieu. We also characterize the role of the ER in transferring Ca^{2+} to other stores. We propose a model in which the ER is the distribution center for Ca^{2+} and due to the high Ca^{2+} affinity of the SERCA Ca^{2+}-ATPase the ER is highly efficient at storing Ca^{2+} and transferring it to other compartments.

RESULTS

Extracellular Ca^{2+} predominantly fills the endoplasmic reticulum and acidic stores

We first set up experiments to follow the destination of Ca^{2+} taken up by extracellular tachyzoites from the extracellular milieu into their cytosol. Tachyzoites were loaded with the ratiometric Ca^{2+}

105 indicator Fura-2 and incubated in Ringer buffer containing 100 µM EGTA to chelate extracellular
106 Ca^{2+}, preventing its uptake, and investigated the release of intracellular Ca^{2+} pools by different
107 inhibitors.
108 When thapsigargin (TG), which inhibits the activity of SERCA, was added, it prevented the
109 re-uptake of Ca^{2+} into the ER and unmasked the leakage of Ca^{2+} from the ER into the cytosol,
110 causing a Ca^{2+} cytosolic increase of approximately 160 nM **(Fig. 1B and S1A)**. We compared this
111 with the effect of ionomycin (IO), a Ca^{2+}/H^{+} ionophore which acts on neutral intracellular Ca^{2+}
112 stores, inducing depletion of Ca^{2+}, mainly from the ER (Smith *et al.*, 1989). Exposure of *T. gondii*
113 to 1 µM ionomycin caused a cytosolic increase of approximately 700-1100 nM Ca^{2+} (**Fig. S1A-**
114 **B**). We next tested another SERCA inhibitor, cyclopiazonic acid (CPA), with a different mode of
115 action than TG. CPA caused a lower Ca^{2+} cytosolic increase than the one caused by TG, possibly
116 implying less specificity toward TgSERCA **(Fig. S1B).** Exposure of parasites to TG before CPA
117 ablated CPA's effect, but this did not occur when adding CPA prior to TG **(Fig. S1C-D)**. Although
118 TG does a better job at depleting the ER of Ca^{2+}, the increase of cytosolic Ca^{2+} after adding TG is
119 un-impressive when compared to the effect of IO **(Fig. S1A)**. This result could indicate the
120 presence of other calcium stores not inhibited by TG or simply that TG was not very efficient at
121 blocking TgSERCA.
122 Next, we tested the effect of Ca^{2+} entry in the filling of intracellular stores by measuring the
123 cytosolic Ca^{2+} increases in response to inhibitors after pre-exposing the parasite suspension to
124 extracellular Ca^{2+} (**Fig. 1C-F,** *dark traces*). Addition of 1.8 mM Ca^{2+} caused a cytosolic increase
125 due to influx through a partially characterized plasma membrane pathway (**Fig. 1C**, *dark blue*
126 *trace*) (Pace *et al.*, 2014). This Ca^{2+} influx appeared to be immediately taken up by the ER as the
127 response to TG was much greater in parasites previously exposed to extracellular Ca^{2+} (compare
128 light and dark blue traces) (**Fig. 1C**). We next tested the lysosomotropic agent glycyl-L-
129 phenylalanine-naphthylamide (GPN), which mobilizes Ca^{2+} from acidic organelles (Haller *et al.*,
130 1996; Lloyd-Evans *et al.*, 2008; Miranda *et al.*, 2010; Yuan *et al.*, 2021) and observed a similar
131 pattern (**Fig. 1D**). The cytosolic Ca^{2+} increase upon addition to GPN in parasites previously
132 exposed to extracellular Ca^{2+} was much greater than in cells not exposed to extracellular Ca^{2+} (**Fig.**
133 **1D**, *compare light and dark blue traces*). A similar phenomenon was observed when adding
134 nigericin (acting on acidic stores) or CCCP (most likely acting on mitochondria) (**Figs 1E-F**, *dark*
135 *purple and orange traces, respectively*). These data indicate that the ER, mitochondrion, and
136 PLVAC and other acidic stores, all appear to have the ability to access extracellular Ca^{2+}. The ER
137 displayed the highest capacity to access a large portion of extracellular Ca^{2+}, with TG inducing
138 close to ~500-900 nM of Ca^{2+} release after pre-exposure to Ca^{2+} and only 210 nM Ca^{2+} without
139 Ca^{2+} pre-exposure **(Fig. 1C)**.
140 In summary, upon pre-exposure of *T. gondii* to physiological levels of extracellular Ca^{2+}, the
141 ER, mitochondria, and acidic stores exhibited the capacity to release many times more Ca^{2+} than
142 without pre-exposure, with the ER and GPN-sensitive stores displaying the greatest response **(Fig**
143 **1G).**

144 We next hypothesized that if the ER is the most efficient organelle to access extracellular Ca^{2+}
145 and pass it to the other organelles, it should be possible to see an increased response to agonists
146 like GPN and nigericin after inhibiting SERCA with TG permitting the buildup of Ca^{2+} on the
147 cytosolic side of the ER membrane. For the next experiment we added Ca^{2+} to fill the stores,
148 followed by TG to cause Ca^{2+} efflux from the ER, and then GPN (**Fig. 1H**). We compared the
149 response to GPN between plus and minus the addition of TG and observed that the cytosolic
150 increase caused by GPN when preceded by TG was significantly larger (**Fig. 1H**). We followed
151 the same approach with nigericin and observed that the response increased after the addition of
152 TG (**Fig. 1I**). These experiments support our hypothesis that extracellular Ca^{2+} is used to fill the
153 ER and from the ER Ca^{2+} can be distributed to other organelles.
154

155 **Ca^{2+} uptake by the SERCA-Ca^{2+} ATPase in permeabilized tachyzoites**

156 The previous results highlighted an important role for the ER in taking up Ca^{2+} from the
157 cytoplasm after an increase due to influx from the extracellular milieu. We believe that this ER
158 uptake, essential for keeping stores filled with Ca^{2+}, is due to the high Ca^{2+} affinity of TgSERCA.
159 The SERCA functions as an essential mechanism for the ER to maintain its Ca^{2+} levels, an
160 especially important function considering the leakage of Ca^{2+} from the ER into the cytosol which
161 occurs constitutively and passively (Camello *et al.*, 2002).
162 We developed a protocol that allowed us to measure directly Ca^{2+} uptake by the store where
163 the SERCA is localized (ER), based in the compartmentation of a fluorescent dye in permeabilized
164 cells. We used the low affinity indicator MagFluo4 which has a Kd for Ca^{2+} of 22 μM (Rossi and
165 Taylor, 2020). The cytosolic concentration of Ca^{2+} in *T. gondii* is around ~70 nM (Moreno and
166 Zhong, 1996), which is considerably below the detection limit of MagFluo4. We loaded parasites
167 for an extended length of time and using high concentrations of MagFluo4-AM as the intention
168 was for the indicator to compartmentalize. At the end of the incubation, parasites were washed and
169 exposed to low concentration of digitonin, which permeabilized the plasma membrane leaving the
170 organellar membranes intact. Under these conditions we had parasites loaded with a Ca^{2+} indicator
171 inside organelles (**Fig. 2A**). We next determined the capacity of these permeabilized parasites to
172 take up Ca^{2+}. SERCA activity is dependent on the presence of Mg-ATP (**Fig. 2B**) and we added
173 this substrate under defined concentrations of Ca^{2+} (determined using the MaxChelator program).
174 (Bers *et al.*, 1994). We observed that under these conditions a consistent and reproducible Ca^{2+}
175 uptake was measured that was optimal at 220 nM Ca^{2+} and 500 μM MgATP (**Figs 2B-C**).
176 Validation that this activity was due to SERCA is shown in the experiment in which we added TG
177 highlighting the ER Ca^{2+} leakage (**Fig. 2D**). Note that the Ca^{2+} released by TG appears to be modest
178 but the Kd of the indicator is 22 μM so a small decrease is highly significant when considering the
179 amount of Ca^{2+} that it represents. Ionomycin can be more effective and larger amounts of Ca^{2+}
180 were released from the ER and other stores as the minimum reached is lower than the starting level
181 of Ca^{2+} (**Fig. 2E**).
182 In summary, these results showed that we can measure SERCA activity *in situ* in permeabilized
183 parasites with the low affinity Ca^{2+} indicator MagFluo4. This activity is dependent on MgATP and

184 TG causes release of the accumulated Ca^{2+}. The better effect of IO could be due to Ca^{2+} release
185 from other compartments driven by other ATPases (TgA1).
186
187 **TgSERCA and the *T. gondii* lytic cycle**

188 To investigate the role of TgSERCA (TGGT1_230420) in the biology of *T. gondii* we created
189 conditional KOs (*iΔTgserca*) by inserting a tetracycline regulatable element at the 5' end of the
190 gene to control the expression of the gene with ATc (Sheiner *et al.*, 2011). In addition, we
191 endogenously tagged TgSERCA with HA. We isolated clonal cell lines of *iΔTgserca* and clones
192 expressing *iΔTgserca-HA* (**Fig. 3A**). Western blots (**Fig. 3B**) and immunofluorescence analysis
193 (**Fig. S2**) showed that the expression of TgSERCA is tightly regulated by ATc and it is absent after
194 1.5 days in culture. The growth of the *iΔTgserca* was severely retarded when cultured in the
195 presence of ATc as evaluated by plaque assays (**Fig. 3C-D**). In this assay, parasites engage in
196 repetitive cycles of invasion, replication, and egress causing host cell lysis and formation of
197 plaques in confluent monolayers infected with *T. gondii*. Replication was severely impacted after
198 down regulation of SERCA, and parasites were unable to proceed after one or two replication
199 cycles (**Fig 3E-F**). All (100%) PVs of the ATc cultured mutant contained 4 parasites or less (**Fig.
200 3F**, *bar graph on the right*). Invasion of host cells was also reduced in the *iΔTgserca* (+ATc)
201 mutant (**Fig. 3G**) and egress stimulated by ionomycin, or natural egress followed pre-incubation
202 with Compound 1, was significantly decreased. Interestingly, when testing egress after the addition
203 of saponin in the presence of extracellular Ca^{2+}, we observed that the tachyzoites egressed sooner
204 (**Fig. 3H**, *saponin egress*). This could be because as the SERCA is not active, the cytosolic Ca^{2+}
205 increase due to Ca^{2+} influx from the extracellular milieu after saponin permeabilization cannot be
206 compensated. In addition, the natural efflux from the ER would result in a higher cytosolic Ca^{2+}
207 increase that would cause a faster egress.
208
209 **Ca^{2+} uptake by the SERCA-ATPase is essential for filling acidic Ca^{2+} stores**

210 The *iΔTgserca* mutant showed a low response to TG (**Fig. 4A**), when measuring cytosolic calcium
211 (**Fig. 4A**) which was also the case when adding TG after extracellular calcium to fill the store (**Fig.
212 4B**). This was most likely the result of the lower activity of TgSERCA. Note that the change in
213 Ca^{2+} in Fig. 4A (*TatiΔku80* cells) is larger than in Fig. 1B (RH strain) and we believe that the
214 difference is related to the characteristics of each cell line (RH vs TatiΔku80). In addition, Mg-
215 ATP-driven Ca^{2+} uptake by permeabilized cells measured with MagFluo4 showed no TgSERCA
216 activity after 48 h of culture with ATc (**Fig. 4C**). This experiment validated the MagFluo4
217 approach for determination of SERCA activity. At 24 hours after culturing the parasites with ATc
218 there was still some SERCA activity (Fig. 4C). Ca^{2+} entry measured in Fura2 loaded *iΔTgserca*
219 (±ATc) parasites was not affected by the downregulation of TgSERCA (**Fig. 4D**). Interestingly,
220 the cytosolic resting Ca^{2+} concentration was not affected in the *iΔTgserca* (+ATc) mutant (Fig. 4
221 A,B, D-H) pointing to a critical role of the plasma membrane Ca^{2+} pump in the homeostasis of
222 cytosolic Ca^{2+}. The response to Zaprinast was diminished but was still present (**Fig 4E**) indicating

223 that Zaprinast acts by releasing Ca^{2+} from the ER and from an additional compartment. Adding
224 Zaprinast after calcium also resulted in a reduced response in the mutant pre-incubated with ATc
225 (**Fig 1F**). We next tested GPN, which acts mostly on acidic stores and the response was also
226 decreased (**Fig. 4G**). Adding GPN after replenishing the cells with Ca^{2+} resulted in an increased
227 response as we showed in Fig. 1, but this response was also reduced when the mutant was grown
228 with ATc (**Fig. 1H**). These results support a link between the stores on which GPN is acting upon
229 and the ER. Considering that downregulation of SERCA impacted the ER storage of Ca^{2+} but did
230 not affect cytosolic Ca^{2+} uptake, the diminished response to GPN, supports that the Ca^{2+}
231 released/leaked from the ER plays an important role in filling the GPN's targeted store.
232
233 **The mitochondrion takes up Ca^{2+} from the ER**

234 In mammalian cells, the high concentration of Ca^{2+} in the ER is important for the production of
235 mitochondrial ATP (Wenzel *et al.*, 2022). This is because of the close proximity between the ER
236 and mitochondria which allows for the directional flow of Ca^{2+} from the ER to the mitochondria
237 (Gincel *et al.*, 2001; Rapizzi *et al.*, 2002). With the aim of determining if the *T. gondii*
238 mitochondria can take up calcium, we introduced a genetic Ca^{2+} indicator in the mitochondrion of
239 *T. gondii* tachyzoites by attaching the *GCaMP6* gene (Chen *et al.*, 2013) to the mitochondrial
240 targeting signal of the *T. gondii* superoxide dismutase 2 (SOD2) gene (Pino *et al.*, 2007) and
241 isolated parasite clones (*Tgsod2gcamp6*) (Vella *et al.*, 2020). GCaMP6 was localized to the
242 mitochondria as detected by Fluorescence (**Fig 5A**). Direct Ca^{2+} uptake was observed in digitonin
243 permeabilized parasites incubated in the presence of increasing concentrations of Ca^{2+} (**Fig 5B-C**).
244 A measurable increase was observed but very high concentrations of Ca^{2+} were needed (**Fig. 5B-**
245 **C**) indicating that the *T. gondii* mitochondria can take up Ca^{2+} but with very low affinity and that
246 the concentrations of Ca^{2+} needed for the uptake were much higher than the concentrations of
247 cytosolic Ca^{2+} that are present in the cytosol of a live cell (**Fig 5B**).
248 We reasoned that the mitochondrion could be taking up Ca^{2+} through close membrane contacts
249 with the ER as it is possible that the concentration of Ca^{2+} in those microdomains could reach
250 much higher levels than in the cytosol and would allow for mitochondrial uptake. We next loaded
251 the *Tgsod2gcamp6* mutant with Fura2 and measured, first, if adding extracellular Ca^{2+} to the
252 parasite suspension led to an increase in GCaMP6 fluorescence. Parallel experiments looking at
253 cytosolic and mitochondrial Ca^{2+} showed that adding extracellular Ca^{2+} does result in an increase
254 in the cytosol, however mitochondrial Ca^{2+} was not affected (**Fig. 5D-E**). We next added TG
255 followed by Ca^{2+} and this led to an increase in cytosolic Ca^{2+} but only TG resulted in a measurable
256 increase in fluorescence of the mitochondrial indicator (**Fig 5G**). Our interpretation is that after
257 adding TG, there was accumulation of Ca^{2+} at the outer side of the ER membrane leading to an
258 increased concentration of the ion which activated mitochondrial uptake.
259 We next inserted the *SOD2GCaMP6* chimeric gene in the *iΔTgserca* mutant and isolated the
260 clonal mutant *iΔTgserca-sod2gcamp6.* We first looked at mitochondrial uptake after adding TG
261 and as shown previously, the parasites cultured without ATc showed a measurable and consistent
262 increase in GCaMP fluorescence after adding TG (**Fig. 5H**, *blue trace*). This was abolished in cells

263 cultured in the presence of ATc as the low expression of TgSERCA would result in the ER
264 depletion of Ca^{2+} (**Fig. 5H,** *pink trace*). Interestingly, we observed an increase in the GCaMP
265 fluorescence after adding GPN, ionomycin or Zaprinast (**Fig. 5H-J,** *blue traces*). In all cases the
266 fluorescence increase was muted in the *iΔTgserca* (+ATc) and the difference in the response was
267 always significant (**Fig. 5H-J,** *pink traces*).
268 In summary, we demonstrated that the mitochondrion of *T. gondii* can take up Ca^{2+} through its
269 transfer from the ER, a phenomenon that becomes evident after blocking the ER uptake with TG
270 as the concentration of Ca^{2+} needed to activate the uptake is very high and only reachable at
271 membrane contact sites between the ER and mitochondria. The *iΔTgserca* (+ATc) mutant, is
272 unable to keep the ER filled with Ca^{2+} and this impacts the capacity of the mitochondria to take up
273 Ca^{2+}. The mitochondria could be also taking up Ca^{2+} directly from acidic stores, which became
274 depleted when TgSERCA was downregulated.
275
276 **Interaction between the ER and the mitochondrion and acidic compartments.**
277 We next investigated if it was possible to see interaction between the ER with other organelles by
278 IFA and/or EM. We performed IFAs with ER and mitochondria markers and ER and PLVAC
279 markers (**Fig. 6**). We observed that in intracellular parasites the mitochondrion surrounds the ER
280 and multiple potential points of interaction are seen (**Fig. 6A** and supplemental video 1). The
281 mitochondrion of intracellular *T. gondii* tachyzoites surrounds the periphery of the cell in a lasso-
282 shape morphology. In extracellular parasites the mitochondrion changes drastically its shape
283 adopting either a sperm-like or a collapsed conformation (Ovciarikova *et al.*, 2017) (**Fig. 6B** and
284 supplemental video 2). Our hypothesis is that this retraction of the mitochondrion allows the ER
285 to expand in extracellular parasites into ER tubules, which extend toward the apical domain of the
286 parasite where Ca^{2+} is needed for secretion of micronemes and conoid extrusion.
287 The PLVAC also showed points of contact with the ER (**Fig. 6C** and supplemental video 3).
288 Multiple points of contact were also observed by EM between the ER and the PLVAC, the ER and
289 the apicoplast and the ER and the mitochondrion (**Fig. 6D**).
290 Interestingly these contacts were still present in the *iΔTgserca* (+ATc) mutant (**Fig. S3, A-D**),
291 as most likely TgSERCA would not be directly involved in the establishment of contacts. We
292 quantified the length of the limiting membrane of the organelle in contact with ER tubules at a
293 distance of less than 30 nM and found that after knockdown of TgSERCA, the contact was not
294 altered. However, Calcium transported from the ER into the mitochondrion after thapsigargin
295 treatment was significantly decreased which means that this phenotype is due to reduced ER
296 Calcium and not to lack of contacts (**Fig. S3E**). A similar result was seen when measuring contacts
297 between the ER and the apicoplast (**Fig. S3F**) and between the ER and the PLVAC (**Fig. S3G**).
298 In summary, this data showed that the ER form contacts with other organelles like the
299 mitochondrion, the PLVAC and the apicoplast and these contacts could be the ones allowing the
300 transfer of Calcium from the ER, the store with the highest amount of Calcium, to the other
301 organelles. The SERCA high affinity for Calcium is critical for the filling of the ER. However, the
302 molecular mechanisms involved in the uptake by the other organelles is less clear. Very little is

303 known about the structure and composition of Membrane Contact Sites in *T. gondii* (Huet and
304 Moreno, 2023). However, functional evidence for the transfer of Calcium has been demonstrated
305 for the ER-apicoplast (Li *et al.*, 2021) and in this work we presented evidence for the transfer of
306 Calcium between the ER and the mitochondrion and the ER and the PLVAC.
307
308 **DISCUSSION**

309 In this work we showed that the endoplasmic reticulum (ER) of *T. gondii* has an impressive
310 capacity for capturing Ca^{2+} that enters the cytosol from the extracellular milieu, and it
311 accomplishes this with a minimal increase in cytosolic Ca^{2+} levels. This is the result of a highly
312 efficient SERCA Ca^{2+}-ATPase (TgSERCA) which also showed high affinity for Ca^{2+}. The
313 TgSERCA activity combined with the plasma membrane Ca^{2+} pump (Luo *et al.*, 2001; Luo *et al.*,
314 2005) would not allow the cytosolic Ca^{2+} to increase above 200 nM (Hortua Triana *et al.*, 2024).
315 We also provide evidence of the ER's capacity for sharing Ca^{2+} with other organelles, which
316 originates from the ER unique ability to capture a sizable portion of extracellular Ca^{2+}. We showed
317 that extracellular Ca^{2+} can be efficiently taken up into the ER through the activity of SERCA and
318 from the ER it can be transferred to other compartments like the mitochondria and acidic stores.
319 These activities would ensure that Ca^{2+} is released at specific locations without flooding the whole
320 cell with Ca^{2+}, which may trigger unnecessary signals. Although initial data suggested a less
321 important role for the mitochondria and PLVAC in Ca^{2+} storage, our results showed that these
322 organelles may become more relevant Ca^{2+} reservoirs during ER calcium overload
323 The SERCA Ca^{2+}-ATPase is a P-type ATPase found in the membranes of the ER and the
324 secretory pathway (Kuhlbrandt, 2004). The mammalian genome encodes for three SERCA pumps:
325 SERCA1, SERCA2, and SERCA3, and seven different isoforms expressed from these genes,
326 SERCA1a/1b, SERCA2a/2b, and SERCA3a/3b/3c (Periasamy and Kalyanasundaram, 2007).
327 SERCA2b is the most widespread of all isoforms and phylogenetically likely the oldest and
328 considered the house-keeping isoform (Wuytack *et al.*, 2002). SERCA pumps translocate two Ca^{2+}
329 ions and hydrolyze one ATP for each catalytic turnover. This pumping activity serves several roles.
330 By translocating Ca^{2+} from the cytosol into the lumen of the ER, it restores the cytosolic Ca^{2+}
331 concentration to its low resting level (<100 nM). The stored Ca^{2+} can be released and activate
332 many cellular activities. In addition, SERCA maintains a sufficiently high (~500 μM) luminal Ca^{2+}
333 concentration that is necessary for enzyme activities important for proliferation, growth, and
334 differentiation (Wuytack *et al.*, 2002).
335 *T. gondii* appears to express a single SERCA protein (TgSERCA) (Nagamune and Sibley, 2006),
336 most likely playing a housekeeping role like the mammalian SERCA2. This was evident from the
337 strong phenotype of the *iΔTgserca* (+ATc) mutant, which could not replicate after 24 h and was
338 defective for all the steps of the tachyzoite lytic cycle. The activity of TgSERCA was highly
339 dependent on the presence of its substrate MgATP and it showed high affinity for Ca^{2+}.
340 Considering the low affinity of the indicator Magfluo4 (Kd: 22 μM), the measured uptake activity
341 and the accumulation of Ca^{2+} was impressive as it was evident even at 55 nM free calcium. This
342 result signified that TgSERCA is highly efficient at keeping the cytosol at the low 60-100 nM level

343 as well as efficiently filling the ER with Ca^{2+}.
344 Ca^{2+} signals are specifically contingent on their spatial, temporal and amplitude features.
345 Movement of Ca^{2+} in the cytosol of cells is severely limited due to the presence of high affinity
346 Ca^{2+} buffers. The concept of Ca^{2+} tunneling through the ER proposed that Ca^{2+} would move more
347 easily within the lumen of the ER as its binding capacity is almost 100 lower than the binding
348 capacity of the cytosol (Mogami *et al.*, 1997) and the high mobility of Ca^{2+} through the lumen of
349 the ER was directly demonstrated (Park *et al.*, 2000), and especially important in polarized cells.
350 In addition, the ER facilitates Ca^{2+} tunneling through its lumen as a mechanism of delivering Ca^{2+}
351 to targeted sites without activating inappropriate processes in the cell cytosol (Petersen *et al.*,
352 2017). In *T. gondii*, the Ca^{2+} binding capacity of the cytosol compared to the ER is less known as
353 the localization of all its predicted Ca^{2+} binding proteins have not been completely determined and
354 several calmodulin-like proteins showed localization to the conoid (Long *et al.*, 2017).
355 In *T. gondii* cytoplasmic Ca^{2+} increases, due to efflux from the ER, have been reported to initiate
356 essential parasite traits like microneme secretion (Carruthers and Sibley, 1999; Nagamune *et al.*,
357 2007b), conoid extrusion (Del Carmen *et al.*, 2009), invasion (Vieira and Moreno, 2000; Lovett
358 and Sibley, 2003) and egress (Arrizabalaga *et al.*, 2004). These responses require precise
359 spatiotemporal control of diverse targets and suggests the presence of distinct systems to deliver
360 Ca^{2+} to specific locations. Our hypothesis is that the ER plays a central role by distributing Ca^{2+} to
361 those locations at specific times for the initiation of parasite functions. The strong invasion,
362 replication and egress phenotypes of the *iΔTgserca* (+ATc) supports this hypothesis.
363 In mammalian cells Ca^{2+} ion is transferred from the ER to the mitochondrion through the outer
364 membrane voltage-dependent anion channel1 (VDAC1) (Gincel *et al.*, 2001; Rapizzi *et al.*, 2002)
365 and the inner membrane calcium uniporter (MCU1) (De Stefani *et al.*, 2011). A VDAC homologue
366 is present in *T. gondii*, which was shown to be essential for growth and for mitochondrial and ER
367 morphology (Mallo *et al.*, 2021). However, the molecular evidence for the presence of a Ca^{2+}
368 uniporter in the inner mitochondrial membrane driven by the electrochemical gradient generated
369 by the electron transport is not supported by the genome database. Calcium transport into the *T.*
370 *gondii* mitochondrion had not been previously shown and our data represents the first experimental
371 evidence showing this event although the mechanism is less clear. We showed that it has very low
372 affinity for Ca^{2+} and it was only possible to observe it in intact parasites after inhibiting SERCA,
373 which allowed the increase of the concentration of Ca^{2+} at the local ER membrane. Over the past
374 decade a new concept about the communication between subcellular organelles through tight,
375 stable, and yet non-fusogenic associations known as membrane contact sites (MCSs) has emerged
376 (Phillips and Voeltz, 2016). The ER forms an extensive network of MCSs with the PM,
377 mitochondria and endocytic vesicles for the exchange of Ca^{2+} (Burgoyne *et al.*, 2015).
378 In *T. gondii* the characterization of MCSs is only in its beginnings (Huet and Moreno, 2023) with
379 only a few evidences for their presence (Tomova *et al.*, 2009; Mallo *et al.*, 2021; Ovciarikova *et*
380 *al.*, 2022) and function (Li *et al.*, 2021; Oliveira Souza *et al.*, 2022). When *T. gondii* is intracellular,
381 microscopy observations showed that its mitochondrion surrounds the periphery of the cell in a
382 lasso-shape conformation. On the other hand, in extracellular parasites the mitochondrion changes

383 its morphology and adopts a sperm-like or collapsed conformation (Ovciarikova *et al.*, 2017). Our
384 IFA analysis with ER and mitochondrial markers showed that the lasso-shaped mitochondrion
385 surrounds the ER with plenty of opportunities for contact between both organelles. We speculate
386 that at this stage the mitochondrion is buffering any leakage of Ca^{2+} from the ER to prevent
387 premature egress as a cytosolic increase would stimulate motility and possibly egress.
388 In this work, we showed that Ca^{2+} can be transferred from the ER to the mitochondrion, most
389 likely through MCSs as the low affinity of the mitochondrion would not permit uptake directly
390 from the cytosol. Down regulation of TgSERCA resulted in diminished response to acidic stores
391 triggers, which supported that the ER may also be responsible for their filling. The mitochondrion
392 may also be able to take up Ca^{2+} from acidic stores like the PLVAC as GPN was also able to
393 stimulate Ca^{2+} uptake and the response was diminished in the *iΔTgserca* (+ATc) mutant. Transfer
394 of Ca^{2+} from acidic stores to the mitochondrion was impacted by the ER depletion (Fig. 7).
395 In conclusion, this study showed how the ER of *T. gondii* replenish itself with calcium and how
396 it supplies Ca^{2+} to the cytosol for signaling and to acidic stores and the mitochondrion. *T. gondii*
397 is a protozoan parasite that causes disease by reiterating a lytic cycle that is driven by calcium
398 signaling. This work contributes to the understanding of how extracellular and intracellular Ca^{2+}
399 stores work together to sustain the pathologic features of *T. gondii*. Future studies would aim at
400 finding more about the role of Ca^{2+} in mitochondrial and acidic stores functions.
401
402 **Methods**

403 ***Cell Culture***—*Toxoplasma gondii* tachyzoites (RH strain) were maintained in human telomerase
404 reverse transcriptase immortalized foreskin fibroblasts (hTERT) (Farwell *et al.*, 2000) grown in
405 Dulbecco's modified minimal essential media (DMEM) with 1% FBS.
406
407 ***Generation of SERCA mutants***—A promoter insertion plasmid was generated by cloning three
408 PCR fragments into a modified pCR2.1-TOPO vector using Gibson Assembly Cloning Kit (NEB
409 #E5510). One fragment corresponding to the TgSERCA flanking region (predicted
410 promoter/5'UTR) was amplified with primers 1 and 2 (Table S1). The second fragment
411 corresponds to DHFR+T7S4 (Sheiner *et al.*, 2011) and was amplified with primers 3 and 4.
412 Another fragment corresponds to the 5' TgSERCA coding sequence beginning with start codon
413 and was amplified with primers 5 and 6. The vector pCR2.1-TOPO was used, which had only one
414 EcoRI site and it was cut with the enzyme NotI to use as a vector backbone. The promoter insertion
415 plasmid was transfected into the *TatiΔku80* cells and selected with 1 μM pyrimethamine using a
416 "ultra aggressive" screening method. Briefly, 200 μl of the suspension of transfected parasites was
417 added to 10 ml of media and then one to three drops (~65 μl per drop) were inoculated into three
418 24-well plates containing media. The clonal lines created after selection and subcloning were
419 termed *iΔSERCA*.
420 For *in situ* tagging, an approximately 2 kb fragment was amplified from the genomic locus (3'
421 region) of the TgSERCA gene using primers 7 and 8. The fragment was cloned into the pLic-3HA-
422 CAT plasmid (Huynh and Carruthers, 2009) and the construct was linearized with the enzyme

423 NheI for transfection into the *iΔSERCA* mutant. Clonal cell lines were generated after selection
424 with chloramphenicol and subcloning and termed *iΔSERCA-3HA*.
425
426 ***Expression and purification of TgSERCA recombinant protein***—The phosphorylation(P) and
427 nucleotide binding(N) domains of *Tg*SERCA (TGGT1_230420) (nucleotides 1123 to 2415, amino
428 acid residues 375 to 805) were cloned into XmaI and HindIII sites of pQE-80L with primers 13
429 and 14 to create recombinant protein with a N-terminal 6xHis tag. The resulting plasmid was
430 transformed into *Escherichia coli* BL21-CodonPlus competent cells and expression was induced
431 by addition of 0.4 mM isopropyl β-D-1-thiogalactopyranoside (IPTG) for 4 hours at 37ºC. Cells
432 were pelleted and resuspended in equilibration/binding buffer (50 mM Na_3PO_4, 300 mM NaCl, 10
433 mM Imidazole, 8 M Urea, and protease inhibitor cocktail P-8849). The cells were then sonicated
434 for 80 seconds total and centrifuged at 12,000 rpm for 20 mins at 4ºC. The supernatant was filtered
435 through a 0.45 µm membrane and the protein was purified using HisPur Ni-NTA Chromatography
436 Cartridge (Thermo Scientific) following instructions from the manufacturer. Proteins that were
437 unbound were washed off with 12 ml of wash buffer (50 mM Na_3PO_4, 300 mM NaCl, 40 mM
438 imidizole, and 8 M urea), and the recombinant protein was eluted with 5 ml elution buffer (50
439 mM Na_3PO_4 , 300 mM NaCl, 250 mM iImidizole, and 8 M urea). Eluted protein fractions were
440 concentrated and desalted with Amicon Ultra-0.5 mL centrifugal filter (Millipore Sigma).
441
442 ***Anti-TgSERCA antibody generation in Guinea pig***—Two Guinea pigs were each immunized
443 with 0.2 mg of purified recombinant protein mixed with equal volume of Freund's Complete
444 Adjuvant (Sigma F5581), followed by two boosts of 0.1 mg antigen mixed with equal volume of
445 Freund's Incomplete Adjuvant (Sigma F5506) for Guinea pig 1 and three boosts for Guinea pig 2.
446 The resulting antibodies were tested at 1:1000 in western blot against RH lysates and were
447 developed with Alexa Fluor 488 goat anti-Guinea pig (1:1000). The antibodies were compared
448 with Dr. Sibley's mouse anti-SERCA antibody (Nagamune *et al.*, 2007a) to confirm size and
449 purity. The anti-*Tg*SERCA antibodies were then affinity purified.
450
451 ***Cytosolic calcium measurements with Fura-2***—*T. gondii* tachyzoites were loaded with Fura-2
452 AM as previously described (Vella *et al.*, 2020; Stasic *et al.*, 2021). Freshly released tachyzoites
453 were washed twice with buffer A plus glucose (BAG; 116 mM NaCl, 5.4 mM KCl, 0.8 mM
454 $MgSO_4$, 50 mM Hepes, pH 7.3, and 5.5 mM glucose), by centrifugation (706 x *g* for 10 min) and
455 re-suspended to a final density of 1 x $l0^9$ parasites/ml in loading buffer (BAG plus 1.5% sucrose,
456 and 5 µM Fura2 AM). The suspension was incubated for 26 min at 26 °C with mild agitation.
457 Subsequently, the parasites were washed twice (2000 x *g* for 2 min) with BAG to remove
458 extracellular dye, re-suspended to a final density of $1x10^9$ parasites per ml in BAG and kept on
459 ice. For fluorescence measurements, 2 x 10^7 parasites/mL were placed in a cuvette with 2.5 mL of
460 Ringer's buffer without calcium (155 mM NaCl, 3 mM KCl, 1 mM $MgCl_2$, 3 mM NaH_2PO_4, and
461 10 mM Hepes, and 10 mM glucose). Fluorescence measurements were done in a Hitachi F-7000
462 fluorescence spectrofluorometer using the Fura-2 conditions for excitation (340 and 380 nm) and
463 emission (510 nm). The Fura-2 fluorescence response to Ca^{2+} was calibrated from the ratio of
464 340/380 nm fluorescence values after subtraction of the background fluorescence of the cells at

340 and 380 nm as previously described (Grynkiewicz *et al.*, 1985). The Ca^{2+} release rate was defined as the change in Ca^{2+} concentration during the initial 20 s after reagent addition. Delta F was calculated by the difference between the higher calcium peak and basal Ca^{2+}, and recovery was defined as the change of Ca^{2+} concentration after the calcium peak was reached for the subsequent indicated times.

Endoplasmic reticulum Ca^{2+} Measurements in permeabilized T. gondii tachyzoites—Tachyzoites freshly egressed and washed as described above were resuspend to a final density of $1x10^9$ cells/ml in HBS buffer (135 mM NaCl, 5.9 mM KCl, 1.2 mM $MgCl_2$, 11.6 mM HEPES pH 7.3, 1.5 mM $CaCl_2$, 11.5 mM glucose) containing 1 mg/ml BSA, 0.2 mg/ml of pluronic F127 and 20 µM MagFluo4/AM. The suspension was incubated in a 20ºC water bath with mild shaking for 1 h, in the dark. Subsequently, parasites were washed 3 times at 5,000 rpm for 2 min to remove extracellular dye. The pellet was resuspended in 1.8 ml of CLM buffer (20 mM NaCl, 140 mM KCl, 20 mM PIPES, pH 7.0) containing 1 mM EGTA at $1x10^9$ cells/ml. Cells were permeabilized with 44.4 µg/ml digitonin for 10 min. Cells were washed 3 times with CLM containing 1 mM EGTA at 5,000 rpm for 2 min to remove digitonin and resuspended to a final density of $1x10^9$ tachyzoites/ml and kept in ice. For each test, 50 µl ($5x10^7$) of parasite suspension was added to 1.95 ml of CLM containing 1 mM EGTA and 0.375 mM $CaCl_2$ which results in 220 nM free Ca^{2+} as calculated with MaxChelator. Fluorescence was measured with an Hitachi F-7000 fluorescence spectrometer (Excitation at 485 nm and emission at 520 nm). Ratio ($\Delta F/F_0$) was evaluated by measuring the rate of change in fluorescence over 20 s after reagent addition (linear rate).

Strain construction and maintenance—The organelle targeting of GCaMP6f was made by overlapping PCR. The N-terminal mitochondrial targeting sequence of the *T. gondii* SOD2 gene (Pino *et al.*, 2007) was used to target GCaMP6f to the mitochondrion. The Gcamp6f for this construct was amplified by primers 9 and 10 (Table S1). After gel purification of the GCaMP6f and SOD2 sequences, the mitochondria targeting construct was built by overlapping PCR with the purified PCR products as template. This construct was then cloned into the Topo-blunt vector. After the sequence was verified by sequencing, the SOD2-Gcamp6f fragment was removed by BglII and AvrII digestion and cloned into the same restriction sites of the pDT7S4H3 (Sheiner *et al.*, 2011) and pCTH3 (Vella *et al.*, 2020) vectors. The pDT7S4H3-SOD2-GCaMP6f construct was introduced into RH parasites by electroporation. After selection with pyrimethamine, the parasites were sorted by FACS and then subcloned. Clones were selected based on the dynamic range of the response to ionomycin. The pCTH3-SOD2-GCaMP6f was introduced into the *iΔTgSERCA* mutant by electroporation. After selection with chloramphenicol, the parasites were sorted by FACS and then subcloned. The expression of GCaMP6f was verified by live cell imaging, IFA, and western blots. The clone with the largest dynamic range, as evaluated with Ionomycin, was selected to further use.

GCaMP6f fluorescence Measurements—Permeabilized tachyzoites: *T. gondii* tachyzoites expressing SOD2-GCaMP6 were collected and washed 3 times at 5,000 rpm for 2 min. The parasite pellet was resuspended in 1.8 ml of BAG buffer containing 0.1 mM EGTA at $1x10^9$

507 cells/ml. Permeabilization with 44.4μg/ml digitonin for 10 min was done by following the
508 fluorescence of GCaMP6. Cells were washed 3 times with the same buffer at 5,000 rpm for 2 min
509 to remove digitonin, resuspended to a final density of $1x10^9$ parasites/ml and kept in ice. 50 μl
510 ($5x10^7$) of the parasite suspension was mixed with 1.95 ml reaction buffer containing 0.1 mM
511 EGTA.
512 For measurements with intact parasites, they were collected, washed, and resuspended in BAG
513 at $1x10^9$ cells/ml for testing. Measurements were done in a Hitachi 7000 fluorescence spectrometer
514 set at excitation, 485 nm and emission, 509 nm. The ratio ($\Delta F/F_0$) was evaluated by measuring the
515 rate of change in fluorescence over 20 s after reagent addition (linear rate).
516
517 ***Growth, Invasion and Egress assays***—Red-green invasion assays were performed as originally
518 described (Kafsack *et al.*, 2004), modified (Chasen *et al.*, 2017) and adapted to use td-RFP
519 expressing parasites. The number of tachyzoites used was 2 x 10^7, and invasion was for 5 min.
520 Plaque assays were performed as described in (Liu *et al.*, 2014) with modifications. 125
521 tachyzoites were used for infection of confluent six well plates with hTert fibroblasts followed by
522 an incubation time of 10 days prior to fixing and staining with crystal violet.
523 For egress assays, HeLa cells were infected with either parental or *iΔTgSERCA-HA*
524 tachyzoites. *iΔTgSERCA-HA* tachyzoites were grown in HeLa cells in the absence or presence of
525 anhydrous tetracycline for the duration of the infection. Forty-eight hours after infection,
526 parasitophorous vacuoles containing 4-8 parasites were monitored by microscopy after washing
527 with Ringer buffer. $CaCl_2$ was omitted for experiments in the absence of extracellular calcium,
528 and the media was supplemented with 100 μM or 1 mM EGTA to chelate contaminating calcium.
529 For experiments containing $CaCl_2$, 2 mM $CaCl_2$ was added to the calcium-free Ringer buffer right
530 before the addition of the specific triggers. Drugs were added in calcium free Ringer buffer at the
531 concentrations indicated: ionomycin (1 μM), thapsigargin (1 μM), zaprinast (100 μM), saponin
532 (0.01%). Ringer buffer was used as extracellular buffer (EB).
533 For natural egress, the *iΔTgSERCA* mutant expressing td-tomato RFP was used to infect
534 confluent host cell monolayers 36 hours before adding ATc and 1 μM compound 1 (pyrrole 4-[2-
535 (4-fluorophenyl)-5-(1-methylpiperidine-4-yl)-1H-pyrrol-3-yl]pyridine) (Donald *et al.*,
536 2002) dissolved in ethanol and the culture continued for 24 hours. After treating with cpd1 for 24
537 hours, cultures showed full vacuoles which differed from the vehicle treated plates (36 hours
538 cultured plus ATc treatment for 24 hours or 48 hours without ATc), which were fully lysed. The
539 cpd1 media was removed and the synchronized vacuoles were washed twice, and the media
540 replaced with media without cpd1. The plates were then moved to the Prewarmed DeltaVision
541 microscope for observation. After 10 minutes at 37C, egress of the full vacuoles was enumerated.
542 We counted each plate for 1 minute and we counted at least 100 vacuoles per experiment. 3
543 independent biological experiments were conducted and summarized.
544 For replication assays, the hTERT cells were grown on 35 mm Mattek dishes. Each dish was
545 infected with 50,000 tdTomato-expressing parasites. 24 h after the infection the counting of
546 parasites per PV was done in a fluorescence microscope. For each experiment, at least 100 PVs
547 were counted. Results were the average of 3 independents experiments (Li *et al.*, 2021).

548
549 ***Microscopy and western blot analyses*—**Tachyzoites were grown on hTERT cells on cover slips for
550 ~24 hr, washed twice with buffer A with glucose (BAG, 116 mM NaCl, 5.4 mM KCl, 0.8 mM $MgSO_4$,
551 50 mM HEPES, pH 7.2, and 5.5 mM glucose) and fixed with 4% formaldehyde for 1 h, followed by
552 permeabilization with 0.3% Triton X-100 for 20 min, and blocking with 3% bovine serum albumin.
553 IFAs were performed as previously described (Miranda *et al.*, 2010). Fluorescence images were
554 collected with an Olympus IX-71 inverted fluorescence microscope with a Photometrix CoolSnapHQ
555 CCD camera driven by DeltaVision software (Applied Precision, Seattle, WA). Superresolution
556 microscopy was performed using a Zeiss ELYRA S1 (SR-SIM) microscope with a high-resolution
557 Axio observer Z1 inverted microscope stand with transmitted (HAL), UV (HBO,) and high-power
558 solid-state laser illumination sources (405/488/561 nm), a 100x oil immersion objective, and an Andor
559 iXon EM-CCD camera and acquired using the ZEN software (Zeiss) with a SIM analysis module.
560 Rat anti-HA antibody from Roche was used at a dilution of 1:25. Mouse anti-HA antibody from
561 Covance was used at a dilution of 1:200.
562 Western blot analysis was performed as previously described (Liu *et al.*, 2014). Rat anti-HA
563 antibody from Roche was used at a dilution of 1:200. Mouse anti-HA antibody from Covance was
564 used at a dilution of 1:1,000. Secondary goat anti-rat or mouse antibody conjugated with HRP was
565 used at 1:5,000. Mouse anti-α-tubulin at a dilution of 1:5,000 was used for loading control.
566
567 ***Transmission Electron Microscopy***—For ultrastructural observations of intracellular *T. gondii* by
568 thin-section transmission electron microscopy (EM), infected human foreskin fibroblast cells were
569 fixed in 2.5% glutaraldehyde in 0.1 mM sodium cacodylate (EMS) and processed as described
570 (Coppens and Joiner, 2003). Ultrathin sections of infected host cells were stained before examination
571 with a Hitachi 7600 EM under 80 kV. For quantitative measurement of distance between organelles,
572 the closest point between *T. gondii's* organelles and ER membrane was measured using ImageJ and
573 was performed on 47 representative electron micrographs at the same magnification for accurate
574 comparison between organelles
575
576 ***Statistical Analysis***—Statistical analyses were performed by Student's t-test using GraphPad PRISM
577 version 9. Error bars shown represent mean ± SD (standard deviation) of at least three independent
578 biological replicates. Unpaired two tailed t test performed in all comparisons.
579
580 **Acknowledgments**
581 The authors thank Dr. Muthugapatti Kandasamy and the Biomedical Microscopy Core of the
582 University of Georgia for the use of the microscopes. The CTEGD Cytometry Shared Resource
583 Laboratory provided access and training to state-of-the-art flow cytometry analyzers. We would like
584 to thank David Sibley for the generous gift of the mouse SERCA antibody and the plasmid for SERCA
585 expression. This work was supported by the U.S. National Institutes of Health grants AI128356,
586 AI154931 and AI174600 to SNJM and R01AI166921 to IC.
587

References

Arrizabalaga, G., and Boothroyd, J.C. (2004). Role of calcium during Toxoplasma gondii invasion and egress. International journal for parasitology *34*, 361-368.

Arrizabalaga, G., Ruiz, F., Moreno, S., and Boothroyd, J.C. (2004). Ionophore-resistant mutant of Toxoplasma gondii reveals involvement of a sodium/hydrogen exchanger in calcium regulation. J Cell Biol *165*, 653-662.

Bers, D.M., Patton, C.W., and Nuccitelli, R. (1994). A practical guide to the preparation of Ca2+ buffers. Methods Cell Biol *40*, 3-29.

Bisio, H., and Soldati-Favre, D. (2019). Signaling Cascades Governing Entry into and Exit from Host Cells by Toxoplasma gondii. Annu Rev Microbiol *73*, 579-599.

Black, M.W., and Boothroyd, J.C. (2000). Lytic cycle of Toxoplasma gondii. Microbiol Mol Biol Rev *64*, 607-623.

Blader, I.J., Coleman, B.I., Chen, C.T., and Gubbels, M.J. (2015). Lytic Cycle of Toxoplasma gondii: 15 Years Later. Annu Rev Microbiol *69*, 463-485.

Bootman, M.D., and Bultynck, G. (2020). Fundamentals of Cellular Calcium Signaling: A Primer. Cold Spring Harb Perspect Biol *12*.

Borges-Pereira, L., Budu, A., McKnight, C.A., Moore, C.A., Vella, S.A., Hortua Triana, M.A., Liu, J., Garcia, C.R., Pace, D.A., and Moreno, S.N. (2015). Calcium Signaling throughout the Toxoplasma gondii Lytic Cycle: A STUDY USING GENETICALLY ENCODED CALCIUM INDICATORS. J Biol Chem *290*, 26914-26926.

Burgoyne, T., Patel, S., and Eden, E.R. (2015). Calcium signaling at ER membrane contact sites. Biochim Biophys Acta *1853*, 2012-2017.

Camello, C., Lomax, R., Petersen, O.H., and Tepikin, A.V. (2002). Calcium leak from intracellular stores--the enigma of calcium signalling. Cell Calcium *32*, 355-361.

Carruthers, V.B., and Sibley, L.D. (1999). Mobilization of intracellular calcium stimulates microneme discharge in Toxoplasma gondii. Mol Microbiol *31*, 421-428.

Chasen, N.M., Asady, B., Lemgruber, L., Vommaro, R.C., Kissinger, J.C., Coppens, I., and Moreno, S.N.J. (2017). A Glycosylphosphatidylinositol-Anchored Carbonic Anhydrase-Related Protein of Toxoplasma gondii Is Important for Rhoptry Biogenesis and Virulence. mSphere *2*.

Chen, T.W., Wardill, T.J., Sun, Y., Pulver, S.R., Renninger, S.L., Baohan, A., Schreiter, E.R., Kerr, R.A., Orger, M.B., Jayaraman, V., Looger, L.L., Svoboda, K., and Kim, D.S. (2013). Ultrasensitive fluorescent proteins for imaging neuronal activity. Nature *499*, 295-300.

Clapham, D.E. (2007). Calcium signaling. Cell *131*, 1047-1058.

Coppens, I., and Joiner, K.A. (2003). Host but not parasite cholesterol controls Toxoplasma cell entry by modulating organelle discharge. Mol Biol Cell *14*, 3804-3820.

De Stefani, D., Raffaello, A., Teardo, E., Szabo, I., and Rizzuto, R. (2011). A forty-kilodalton protein of the inner membrane is the mitochondrial calcium uniporter. Nature *476*, 336-340.

Del Carmen, M.G., Mondragon, M., Gonzalez, S., and Mondragon, R. (2009). Induction and regulation of conoid extrusion in Toxoplasma gondii. Cell Microbiol *11*, 967-982.

Donald, R.G., Allocco, J., Singh, S.B., Nare, B., Salowe, S.P., Wiltsie, J., and Liberator, P.A. (2002). Toxoplasma gondii cyclic GMP-dependent kinase: chemotherapeutic targeting of an essential parasite protein kinase. Eukaryot Cell *1*, 317-328.

Endo, T., Sethi, K.K., and Piekarski, G. (1982). Toxoplasma gondii: calcium ionophore A23187-mediated exit of trophozoites from infected murine macrophages. Exp Parasitol *53*, 179-188.

Farwell, D.G., Shera, K.A., Koop, J.I., Bonnet, G.A., Matthews, C.P., Reuther, G.W., Coltrera, M.D., McDougall, J.K., and Klingelhutz, A.J. (2000). Genetic and epigenetic changes in human epithelial cells immortalized by telomerase. Am J Pathol *156*, 1537-1547.

Gincel, D., Zaid, H., and Shoshan-Barmatz, V. (2001). Calcium binding and translocation by the voltage-dependent anion channel: a possible regulatory mechanism in mitochondrial function. The Biochemical journal *358*, 147-155.
Grynkiewicz, G., Poenie, M., and Tsien, R.Y. (1985). A new generation of Ca2+ indicators with greatly improved fluorescence properties. J Biol Chem *260*, 3440-3450.
Hager, K.M., Striepen, B., Tilney, L.G., and Roos, D.S. (1999). The nuclear envelope serves as an intermediary between the ER and Golgi complex in the intracellular parasite Toxoplasma gondii. J Cell Sci *112 (Pt 16)*, 2631-2638.
Haller, T., Dietl, P., Deetjen, P., and Volkl, H. (1996). The lysosomal compartment as intracellular calcium store in MDCK cells: a possible involvement in InsP3-mediated Ca2+ release. Cell Calcium *19*, 157-165.
Hortua Triana, M.A., Marquez-Nogueras, K.M., Fazli, M.S., Quinn, S., and Moreno, S.N.J. (2024). Regulation of calcium entry by cyclic GMP signaling in Toxoplasma gondii. J Biol Chem *300*, 105771.
Hortua Triana, M.A., Marquez-Nogueras, K.M., Vella, S.A., and Moreno, S.N.J. (2018). Calcium signaling and the lytic cycle of the Apicomplexan parasite Toxoplasma gondii. Biochim Biophys Acta Mol Cell Res *1865*, 1846-1856.
Huet, D., and Moreno, S.N.J. (2023). Interorganellar Communication Through Membrane Contact Sites in Toxoplasma Gondii. Contact (Thousand Oaks) *6*, 25152564231189064.
Huynh, M.H., and Carruthers, V.B. (2009). Tagging of endogenous genes in a Toxoplasma gondii strain lacking Ku80. Eukaryot Cell *8*, 530-539.
Kafsack, B.F., Beckers, C., and Carruthers, V.B. (2004). Synchronous invasion of host cells by Toxoplasma gondii. Mol Biochem Parasitol *136*, 309-311.
Kuhlbrandt, W. (2004). Biology, structure and mechanism of P-type ATPases. Nat Rev Mol Cell Biol *5*, 282-295.
Li, Z.H., King, T.P., Ayong, L., Asady, B., Cai, X., Rahman, T., Vella, S.A., Coppens, I., Patel, S., and Moreno, S.N.J. (2021). A plastid two-pore channel essential for inter-organelle communication and growth of Toxoplasma gondii. Nat Commun *12*, 5802.
Liu, J., Pace, D., Dou, Z., King, T.P., Guidot, D., Li, Z.H., Carruthers, V.B., and Moreno, S.N. (2014). A vacuolar-H(+) -pyrophosphatase (TgVP1) is required for microneme secretion, host cell invasion, and extracellular survival of Toxoplasma gondii. Mol Microbiol *93*, 698-712.
Lloyd-Evans, E., Morgan, A.J., He, X., Smith, D.A., Elliot-Smith, E., Sillence, D.J., Churchill, G.C., Schuchman, E.H., Galione, A., and Platt, F.M. (2008). Niemann-Pick disease type C1 is a sphingosine storage disease that causes deregulation of lysosomal calcium. Nat Med *14*, 1247-1255.
Long, S., Brown, K.M., Drewry, L.L., Anthony, B., Phan, I.Q.H., and Sibley, L.D. (2017). Calmodulin-like proteins localized to the conoid regulate motility and cell invasion by Toxoplasma gondii. PLoS Pathog *13*, e1006379.
Lourido, S., and Moreno, S.N. (2015). The calcium signaling toolkit of the Apicomplexan parasites Toxoplasma gondii and Plasmodium spp. Cell Calcium *57*, 186-193.
Lovett, J.L., and Sibley, L.D. (2003). Intracellular calcium stores in Toxoplasma gondii govern invasion of host cells. J Cell Sci *116*, 3009-3016.
Luo, S., Ruiz, F.A., and Moreno, S.N. (2005). The acidocalcisome Ca2+-ATPase (TgA1) of Toxoplasma gondii is required for polyphosphate storage, intracellular calcium homeostasis and virulence. Mol Microbiol *55*, 1034-1045.
Luo, S., Vieira, M., Graves, J., Zhong, L., and Moreno, S.N. (2001). A plasma membrane-type Ca(2+)-ATPase co-localizes with a vacuolar H(+)-pyrophosphatase to acidocalcisomes of Toxoplasma gondii. EMBO J *20*, 55-64.

Mallo, N., Ovciarikova, J., Martins-Duarte, E.S., Baehr, S.C., Biddau, M., Wilde, M.L., Uboldi, A.D., Lemgruber, L., Tonkin, C.J., Wideman, J.G., Harding, C.R., and Sheiner, L. (2021). Depletion of a Toxoplasma porin leads to defects in mitochondrial morphology and contacts with the endoplasmic reticulum. J Cell Sci *134*.

Marquez-Nogueras, K.M., Hortua Triana, M.A., Chasen, N.M., Kuo, I.Y., and Moreno, S.N. (2021). Calcium signaling through a transient receptor channel is important for Toxoplasma gondii growth. Elife *10*.

Miranda, K., Pace, D.A., Cintron, R., Rodrigues, J.C., Fang, J., Smith, A., Rohloff, P., Coelho, E., de Haas, F., de Souza, W., Coppens, I., Sibley, L.D., and Moreno, S.N. (2010). Characterization of a novel organelle in Toxoplasma gondii with similar composition and function to the plant vacuole. Mol Microbiol *76*, 1358-1375.

Mogami, H., Nakano, K., Tepikin, A.V., and Petersen, O.H. (1997). Ca2+ flow via tunnels in polarized cells: recharging of apical Ca2+ stores by focal Ca2+ entry through basal membrane patch. Cell *88*, 49-55.

Moreno, S.N., and Zhong, L. (1996). Acidocalcisomes in Toxoplasma gondii tachyzoites. The Biochemical journal *313 (Pt 2)*, 655-659.

Nagamune, K., Beatty, W.L., and Sibley, L.D. (2007a). Artemisinin induces calcium-dependent protein secretion in the protozoan parasite Toxoplasma gondii. Eukaryot Cell *6*, 2147-2156.

Nagamune, K., Moreno, S.N., and Sibley, L.D. (2007b). Artemisinin-resistant mutants of Toxoplasma gondii have altered calcium homeostasis. Antimicrob Agents Chemother *51*, 3816-3823.

Nagamune, K., and Sibley, L.D. (2006). Comparative genomic and phylogenetic analyses of calcium ATPases and calcium-regulated proteins in the apicomplexa. Mol Biol Evol *23*, 1613-1627.

Oliveira Souza, R.O., Jacobs, K.N., Back, P.S., Bradley, P.J., and Arrizabalaga, G. (2022). IMC10 and LMF1 mediate mitochondrial morphology through mitochondrion-pellicle contact sites in Toxoplasma gondii. J Cell Sci *135*.

Ovciarikova, J., Lemgruber, L., Stilger, K.L., Sullivan, W.J., and Sheiner, L. (2017). Mitochondrial behaviour throughout the lytic cycle of Toxoplasma gondii. Sci Rep *7*, 42746.

Ovciarikova, J., Shikha, S., and Sheiner, L. (2022). Nuclear Interactions: A Spotlight on Nuclear Mitochondrial Membrane Contact Sites. Contact (Thousand Oaks) *5*, 25152564221096217.

Pace, D.A., McKnight, C.A., Liu, J., Jimenez, V., and Moreno, S.N. (2014). Calcium entry in Toxoplasma gondii and its enhancing effect of invasion-linked traits. J Biol Chem *289*, 19637-19647.

Papp, S., Dziak, E., Michalak, M., and Opas, M. (2003). Is all of the endoplasmic reticulum created equal? The effects of the heterogeneous distribution of endoplasmic reticulum Ca2+-handling proteins. J Cell Biol *160*, 475-479.

Park, M.K., Petersen, O.H., and Tepikin, A.V. (2000). The endoplasmic reticulum as one continuous Ca(2+) pool: visualization of rapid Ca(2+) movements and equilibration. EMBO J *19*, 5729-5739.

Periasamy, M., and Kalyanasundaram, A. (2007). SERCA pump isoforms: their role in calcium transport and disease. Muscle Nerve *35*, 430-442.

Petersen, O.H., Courjaret, R., and Machaca, K. (2017). Ca(2+) tunnelling through the ER lumen as a mechanism for delivering Ca(2+) entering via store-operated Ca(2+) channels to specific target sites. J Physiol *595*, 2999-3014.

Phillips, M.J., and Voeltz, G.K. (2016). Structure and function of ER membrane contact sites with other organelles. Nat Rev Mol Cell Biol *17*, 69-82.

Pino, P., Foth, B.J., Kwok, L.Y., Sheiner, L., Schepers, R., Soldati, T., and Soldati-Favre, D. (2007). Dual targeting of antioxidant and metabolic enzymes to the mitochondrion and the apicoplast of Toxoplasma gondii. PLoS Pathog *3*, e115.

Rapizzi, E., Pinton, P., Szabadkai, G., Wieckowski, M.R., Vandecasteele, G., Baird, G., Tuft, R.A., Fogarty, K.E., and Rizzuto, R. (2002). Recombinant expression of the voltage-dependent anion channel enhances the transfer of Ca2+ microdomains to mitochondria. J Cell Biol *159*, 613-624.

Rossi, A.M., and Taylor, C.W. (2020). Reliable measurement of free Ca(2+) concentrations in the ER lumen using Mag-Fluo-4. Cell Calcium *87*, 102188.

Sagara, Y., and Inesi, G. (1991). Inhibition of the sarcoplasmic reticulum Ca2+ transport ATPase by thapsigargin at subnanomolar concentrations. J Biol Chem *266*, 13503-13506.

Sheiner, L., Demerly, J.L., Poulsen, N., Beatty, W.L., Lucas, O., Behnke, M.S., White, M.W., and Striepen, B. (2011). A systematic screen to discover and analyze apicoplast proteins identifies a conserved and essential protein import factor. PLoS Pathog *7*, e1002392.

Smith, J.B., Zheng, T., and Lyu, R.M. (1989). Ionomycin releases calcium from the sarcoplasmic reticulum and activates Na+/Ca2+ exchange in vascular smooth muscle cells. Cell Calcium *10*, 125-134.

Spang, A. (2018). The endoplasmic reticulum-the caring mother of the cell. Curr Opin Cell Biol *53*, 92-96.

Stasic, A.J., Dykes, E.J., Cordeiro, C.D., Vella, S.A., Fazli, M.S., Quinn, S., Docampo, R., and Moreno, S.N.J. (2021). Ca(2+) entry at the plasma membrane and uptake by acidic stores is regulated by the activity of the V-H(+) -ATPase in Toxoplasma gondii. Mol Microbiol *115*, 1054-1068.

Thastrup, O., Cullen, P.J., Drobak, B.K., Hanley, M.R., and Dawson, A.P. (1990). Thapsigargin, a tumor promoter, discharges intracellular Ca2+ stores by specific inhibition of the endoplasmic reticulum Ca2(+)-ATPase. Proc Natl Acad Sci U S A *87*, 2466-2470.

Tomavo, S., Slomianny, C., Meissner, M., and Carruthers, V.B. (2013). Protein trafficking through the endosomal system prepares intracellular parasites for a home invasion. PLoS Pathog *9*, e1003629.

Tomova, C., Humbel, B.M., Geerts, W.J., Entzeroth, R., Holthuis, J.C., and Verkleij, A.J. (2009). Membrane contact sites between apicoplast and ER in Toxoplasma gondii revealed by electron tomography. Traffic *10*, 1471-1480.

Vella, S.A., Calixto, A., Asady, B., Li, Z.H., and Moreno, S.N.J. (2020). Genetic Indicators for Calcium Signaling Studies in Toxoplasma gondii. Methods Mol Biol *2071*, 187-207.

Vella, S.A., Moore, C.A., Li, Z.H., Hortua Triana, M.A., Potapenko, E., and Moreno, S.N.J. (2021). The role of potassium and host calcium signaling in Toxoplasma gondii egress. Cell Calcium *94*, 102337.

Vieira, M.C., and Moreno, S.N. (2000). Mobilization of intracellular calcium upon attachment of Toxoplasma gondii tachyzoites to human fibroblasts is required for invasion. Mol Biochem Parasitol *106*, 157-162.

Weiss, L.M., and Dubey, J.P. (2009). Toxoplasmosis: A history of clinical observations. Int J Parasitol *39*, 895-901.

Wenzel, E.M., Elfmark, L.A., Stenmark, H., and Raiborg, C. (2022). ER as master regulator of membrane trafficking and organelle function. J Cell Biol *221*.

Wuytack, F., Raeymaekers, L., and Missiaen, L. (2002). Molecular physiology of the SERCA and SPCA pumps. Cell Calcium *32*, 279-305.

Yuan, Y., Kilpatrick, B.S., Gerndt, S., Bracher, F., Grimm, C., Schapira, A.H., and Patel, S. (2021). The lysosomotrope GPN mobilises Ca(2+) from acidic organelles. J Cell Sci *134*.

FIGURES AND FIGURE LEGENDS:

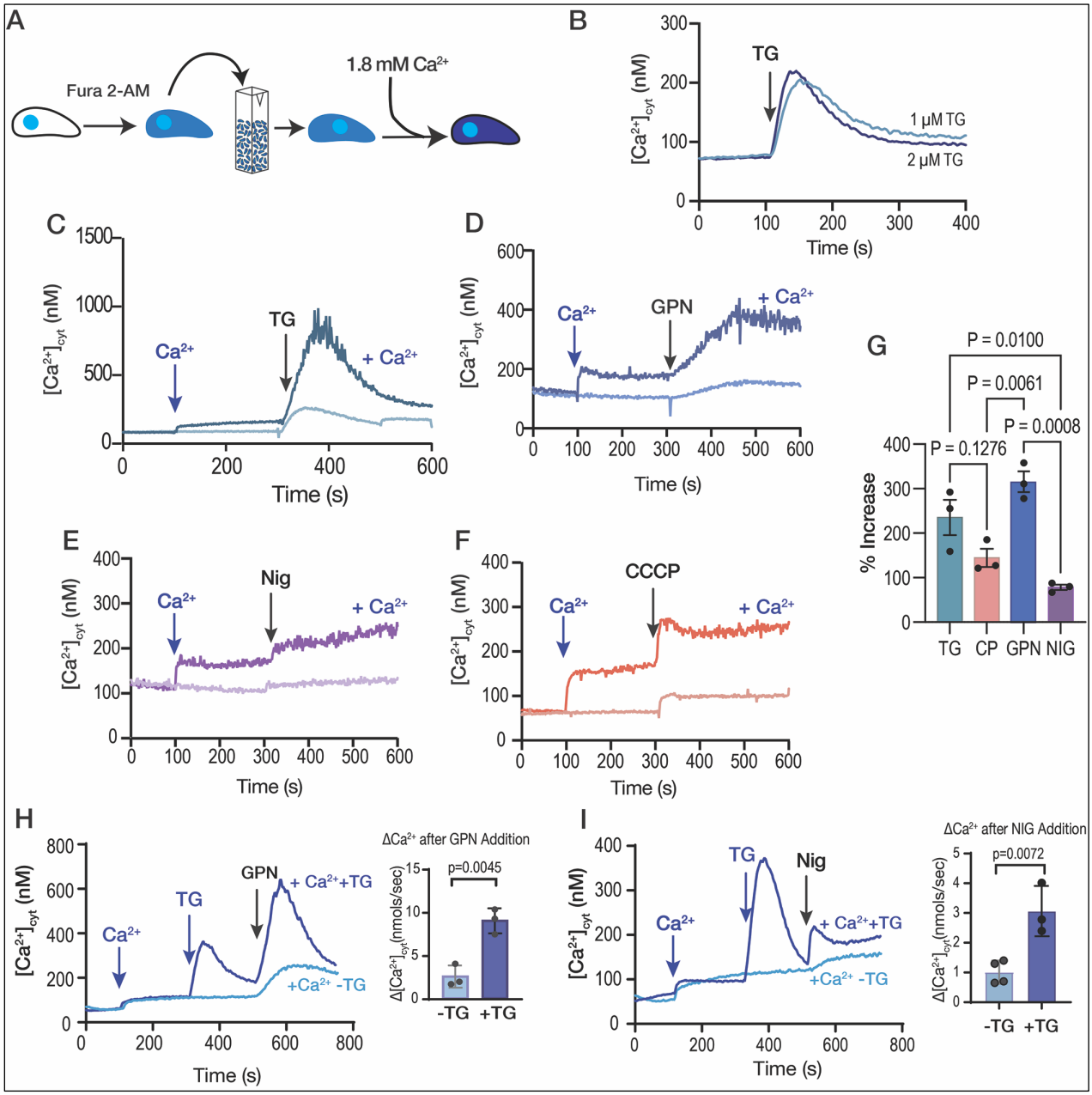

Figure 1: The role of extracellular calcium in the filling of intracellular stores. A, scheme depicting the Fura-2-AM loading and the experimental set-up. **B**, *T. gondii* tachyzoites loaded with Fura-2 were in suspension in Ringer buffer with 100 µM EGTA. Thapsigargin (TG) was added at 100 seconds, at two different concentrations (1 and 2 µM). **C**, Similar experimental set-up to the one shown in B. 1.8 mM $CaCl_2$ was added to the suspension at 100 sec, followed by 2 µM TG at 300 sec (*dark blue trace*). The light blue trace shows the same experiment without the addition of $CaCl_2$. **D**, similar to C but using 40 µM GPN instead of TG. **E**, same experimental set-up to the one shown in C but adding the potassium ionophore nigericin, 10 µM. **F**, same experimental set-up to the one

shown in C but using the mitochondrial uncoupler CCCP. **G**, quantification of the % increase of cytoplasmic calcium by adding extracellular calcium prior to each indicated reagent (TG, thapsigargin; CP, CCCP; NIG, nigericin). **H**, cytosolic calcium measurements following the addition of 1.8 mM extracellular calcium, 1 μM TG prior to the addition of GPN, 40 μM. **I**, cytosolic Calcium measurements following the addition of 1.8 mM extracellular Calcium, 1 μM TG prior to the addition of 10 μM NIG. The quantification shows the comparison of the cytosolic increase with and without the addition of TG. Data are presented as mean ± SD for G, H and I. *p value*: unpaired two tailed t test performed in all comparisons.

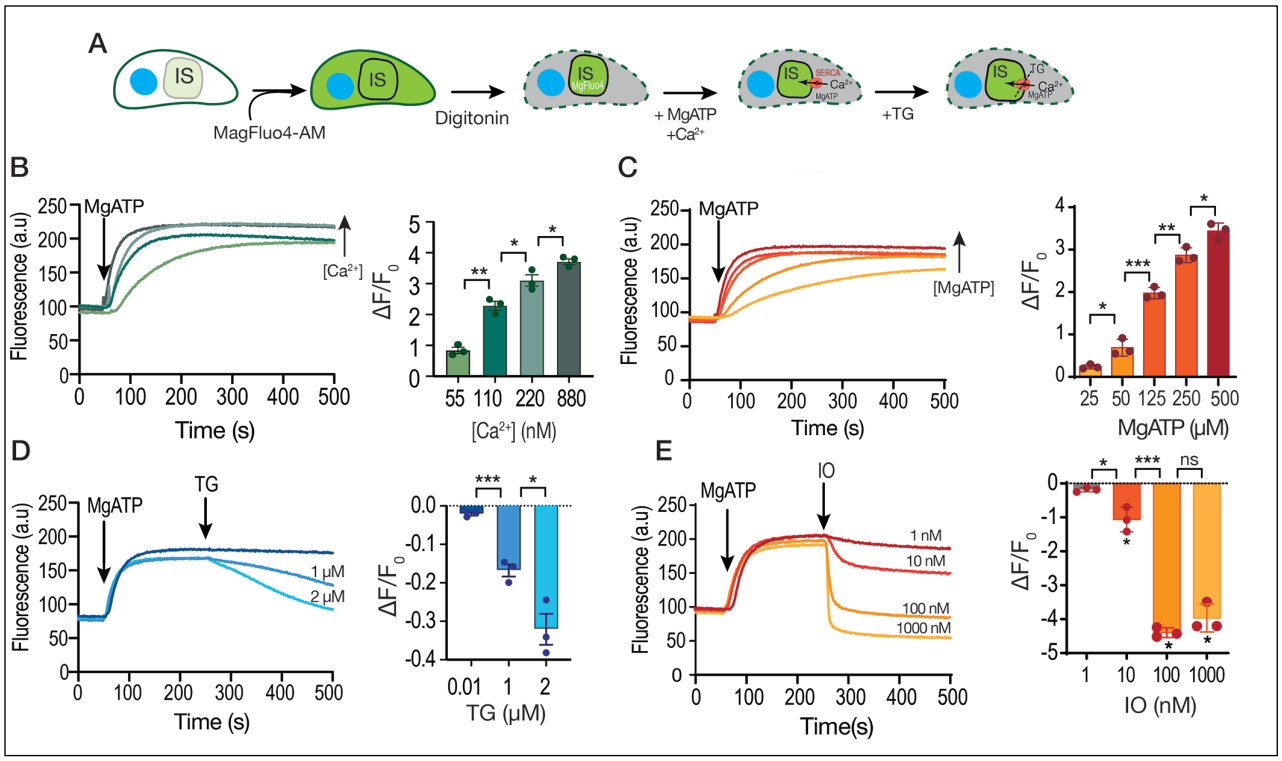

Figure 2: Ca^{2+} uptake by intracellular stores. A, Scheme showing the loading with MagFluo4-AM followed by permeabilization with digitonin of a *T. gondii* tachyzoite (RH parental strain) suspension (IS, intracellular store). **B**, Fluorescence measurements (see Materials and Methods for specifics) of the suspension of parasites loaded with MagFluo4. MgATP was added at 500 μM at 50 seconds. The bar graph shows the quantification of the slope of the increase in fluorescence after adding the SERCA substrate MgATP. The concentration of free calcium was varied, and it is indicated. The calculation of free calcium was done with MaxChelator. **C**, similar experimental set-up to the one shown in B but the concentration of MgATP was varied at the concentrations indicated in the bar graph. Quantification of the slope of fluorescence increase after adding MgATP is shown in the bar graph. **D**, this experiment was done with 500 μM MgATP and 220 nM $CaCl_2$. Thapsigargin (TG) was added to inhibit SERCA causing calcium to be released from the store. The concentrations used are indicated. The bar graph shows the negative slope after the addition of TG. **E**, similar to D, but adding ionomycin (IO). The concentrations used are indicated and the slopes were measured after the addition of IO. Data are presented as mean ± SD for B-D. *p value*: unpaired two tailed t test performed in all comparisons.

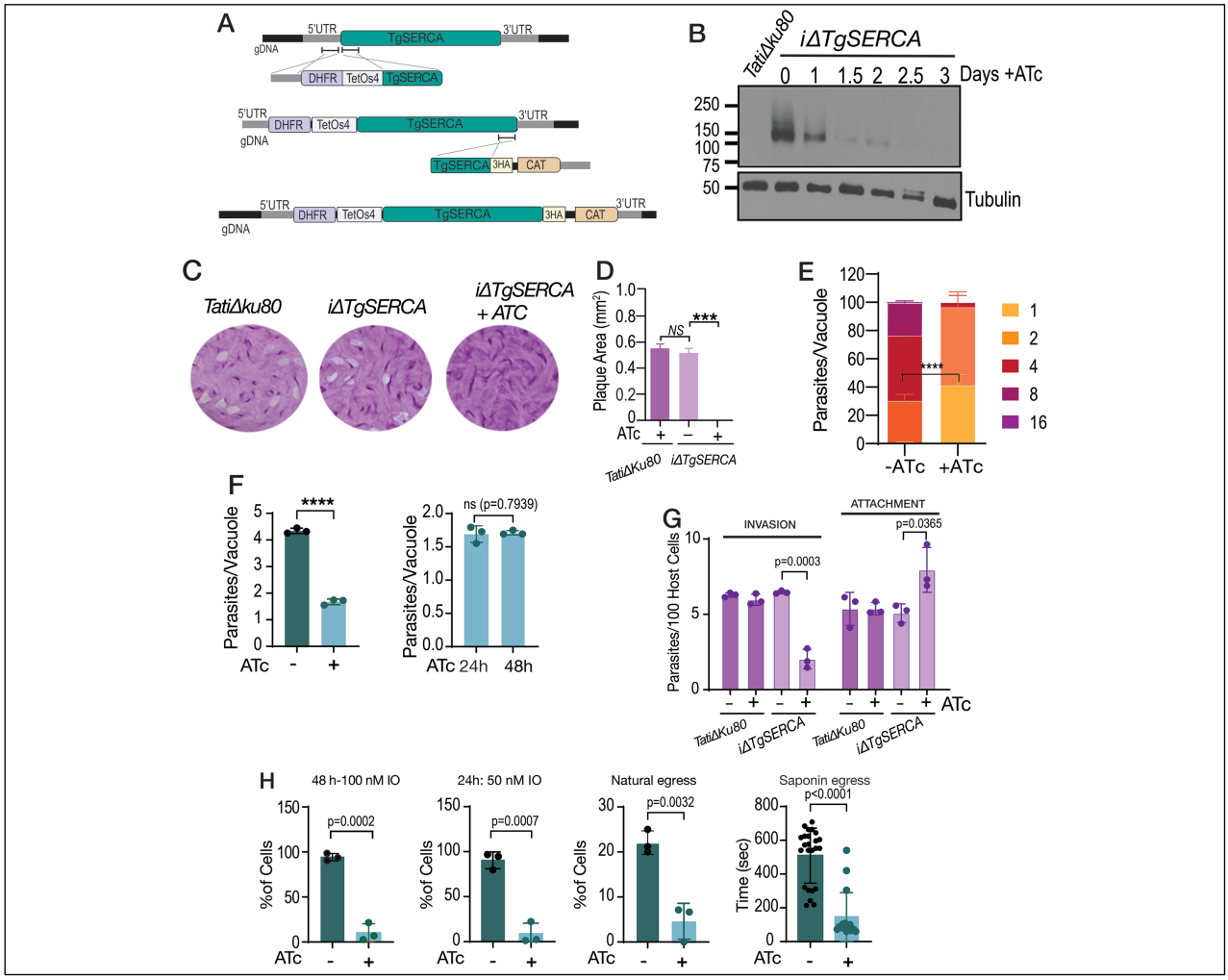

Figure 3: The sarcoplasmic-endoplasmic reticulum calcium ATPase (SERCA) is essential for *T. gondii* replication. A, Scheme showing the strategy used for the down regulation of the expression of TgSERCA by promoter insertion and regulation by 0.5 µg/ml Anhydrotetracyclin (ATc). The mutants generated were termed *iΔTgSERCA* or *iΔTgSERCA-HA* for the C-terminal tagged one. DHFR, Dihydrofolate reductase gene for selection with pyrimethamine; CAT, chloramphenicol acetyl transferase gene for selection with chloramphenicol. **B**, Western blots of *iΔTgSERCA-HA* lysates grown with and without ATc. The expression of TgSERCA is shown by the signal obtained with the anti-HA antibody. **C**, plaque assays comparing the size of plaques formed by tachyzoites (150/well) of the *iΔTgSERCA* mutant grown with and without 0.5 µg/ml ATc for 8 days. Plaques formed by the parental strain *TatiΔku80* are shown for comparison. **D**, quantification of the size of the plaques presented in C. **E**, replication assays using the *iΔTgSERCA_RFP* mutant. Number of parasites per parasitophorous vacuole (PV) obtained 24 h after infection of fibroblast cells is reported and compared between the mutant grown with and without 0.5 µg/ml ATc. Data represented as mean ± SD. *p value*: unpaired two tailed t test performed in all comparisons. **F**, Average number of parasites

per PV counted at 24 h after the initial infection. The graph shown to the right shows the number of parasites per PV of the *iΔTgSERCA* (+ATc) for 24 or 48 hours after the initial infection. **G**, Invasion assays with the *iΔTgSERCA* mutant treated with ATc for 24 h were done using the red-green assay. **H**, Egress assays with the *iΔTgSERCA* mutant previously grown with or without ATc. Egress was triggered with IO (100 or 50 nM) or saponin (0.01%). The protocol for natural egress uses compound 1 and it is detailed in the methods section.

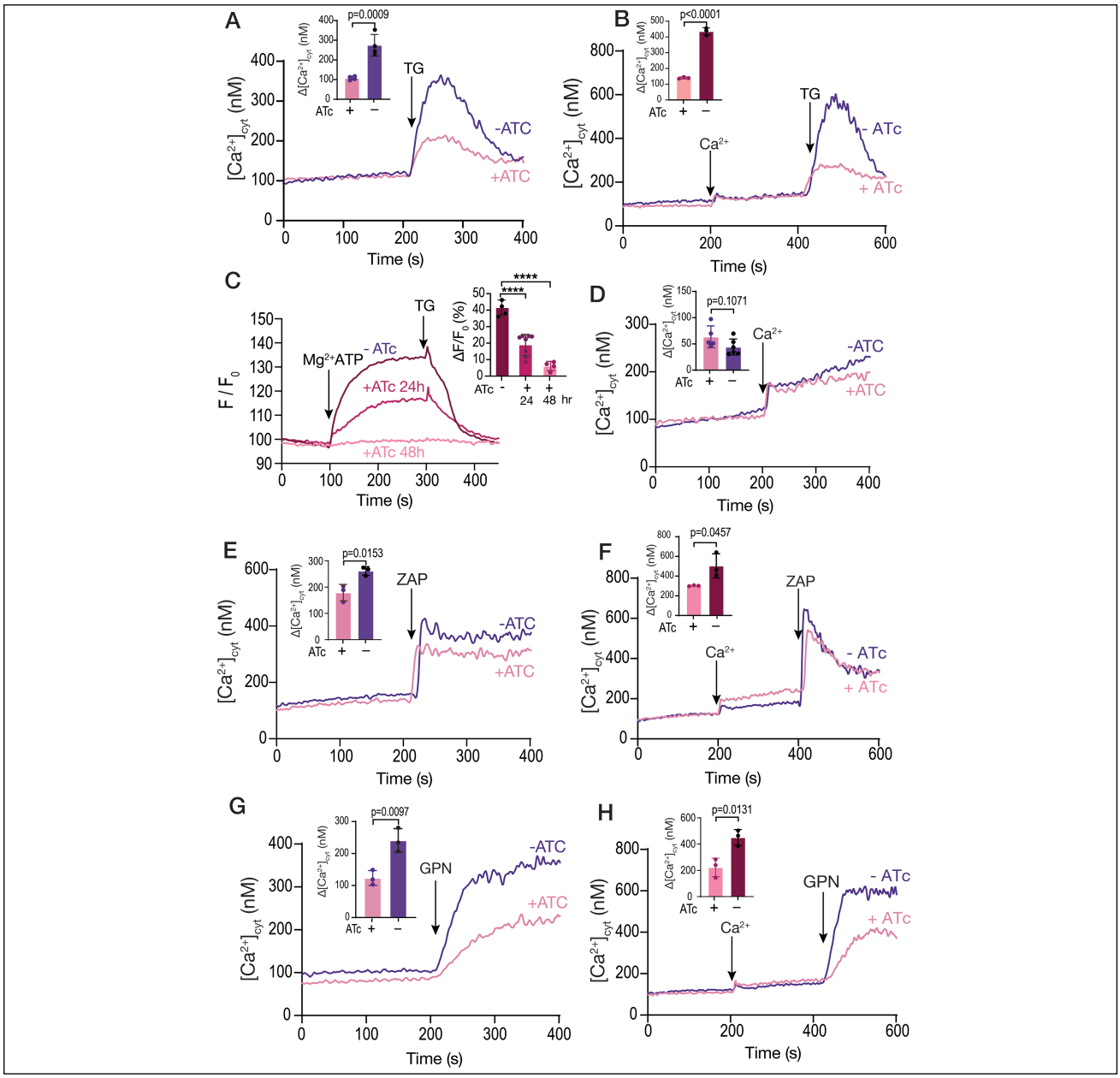

Figure 4: Organellar calcium pools in the *iΔTgserca* mutant. **A**, cytosolic calcium response to the addition of 1 µM TG. The *iΔTgserca* grown with and without ATc was previously loaded with Fura-2 and the cytosolic Ca^{2+} responses were measured. 1 µM TG was added at 200 sec. The purple trace shows the response of the parental cell line grown without ATc and the pink one shows the response of the same mutant grown with ATc for 24 h. The bar graph shows the analysis of the $\Delta[Ca^{2+}]$ from three independent experiments. **B**, same experimental set-up as the one in A but adding 1.8 mM extracellular Ca^{2+} at 200 sec. **C**, SERCA activity measured with MagFluo4-loaded tachyzoites of

iΔTgserca mutant previously grown with or without ATc. Parasites were collected and loaded with MagFluo4-AM as described in the Methods section. Digitonin permeabilized parasites were used in the experiment. The concentration of free calcium in the buffer is 220 nM and MgATP (0.125 mM) was added at 100 sec. The response of the control mutant grown without ATc is shown in purple. The other traces show the response of the mutant grown for either 24 or 48 h with ATc. TG was added at 1 μM TG. The bar graph shows the quantification of the slope after adding MgATP. **D**. Ca^{2+} entry measured in Fura-2 loaded *iΔTgSERCA* (±ATc). 1.8 mM extracellular Ca^{2+} was added at 200 sec. The inset shows the ΔF measurement from three independent experiments and showed no significant difference. **E**, Similar conditions to the ones used in A but adding 100 μM Zaprinast. The bar graph shows the analysis of the $\Delta[Ca^{2+}]$ from three independent experiments. **F**, Similar conditions to the ones used in B but adding 1.8 mM extracellular calcium at 200 sec and 100 μM Zaprinast at 400 sec. The bar graph shows the analysis of the $\Delta[Ca^{2+}]$ from 3 independent experiments. **G**, Same as A but adding 40 μM GPN. The bar graph shows the analysis of the $\Delta[Ca^{2+}]$ from three independent experiments. **H**, Same set-up as in F but adding 1.8 mM Ca^{2+} at 200 sec followed by 40 μM GPN. The bar graph shows the analysis of the $\Delta[Ca^{2+}]$ from three independent experiments. Data are presented as mean ± SD. *p* value: unpaired two tailed t test performed in all comparisons.

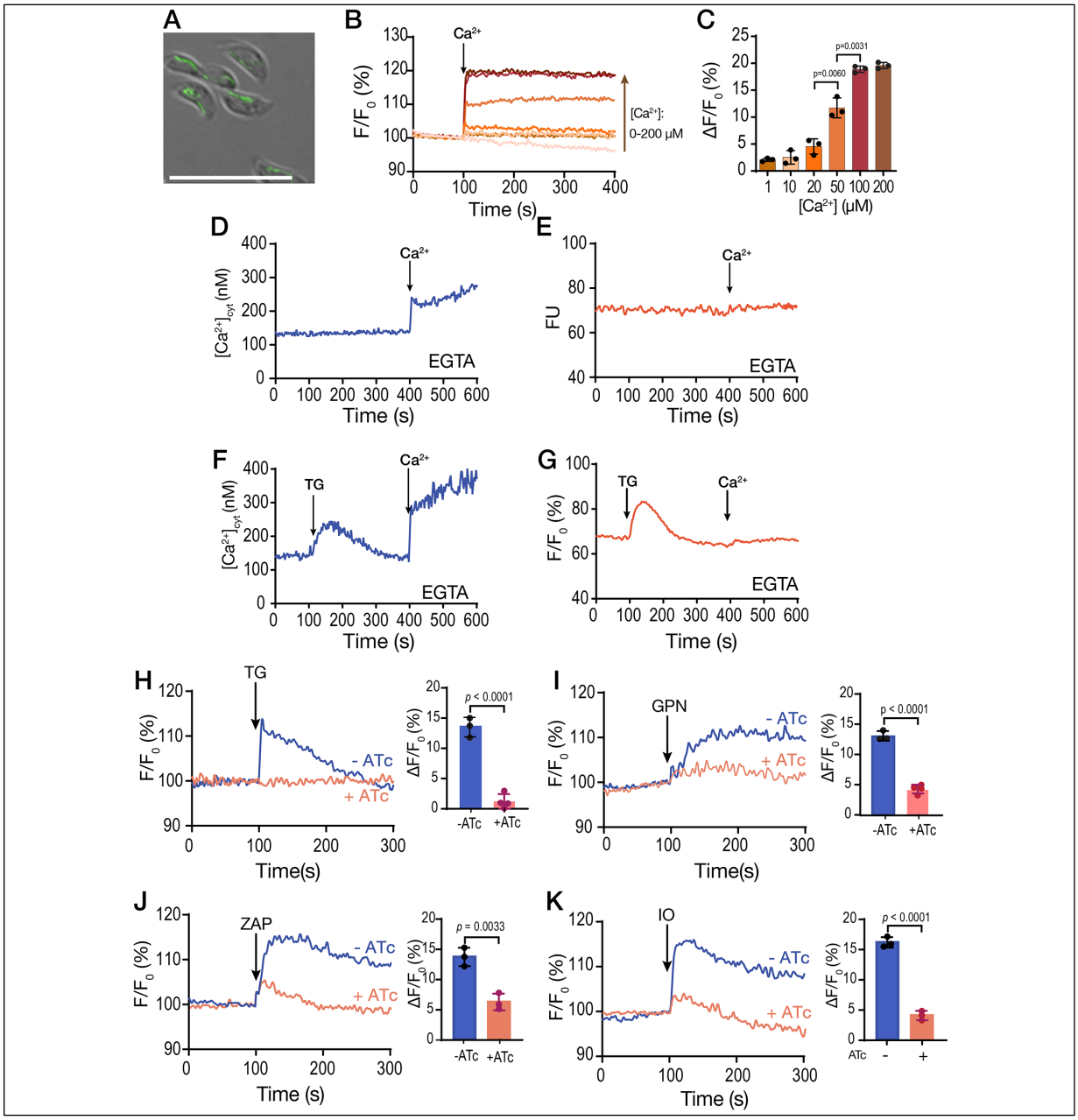

Figure 5: Mitochondrial Calcium uptake. **A**, Fluorescence image of *T. gondii* tachyzoites expressing *SOD2-GCaMP6f* (pDT7S4H3-SOD2-GCaMP6f). The generation of this cell line is described in material and methods. **B**, *T. gondii* tachyzoites expressing SOD2-GCaMP6f ($5x10^7$) permeabilized with digitonin as described in the method's section were tested in a buffer with 100 μM EGTA. Ca^{2+} was added at 100 sec at the final concentrations 1, 10, 20, 50, 100 and 200 μM. Maxchelator was used to calculate the amount of Calcium to be added to attain the indicated concentrations. **C**, ΔF was measured as the change in fluorescence between the baseline and the maximum obtained 20 sec after the addition of Ca^{2+} from three independent biological experiments.

D, Fura-2 loaded tachyzoites of the SOD2-GCaMP6f expressing mutant in suspension. The experimental set-up was identical to the one described in Fig. 1A-B. 1.8 mM $CaCl_2$ was added at 400 sec. Fluorescence measurements were done using the conditions for Fura-2. **E**, GCaMP6 fluorescence measurements of parasites expression SOD2-GCaMP6f in their mitochondrion. The fluorometer conditions were set to measure GCaMP6. **F**, 1 μM TG was added at 100 sec followed by 1.8 mM $CaCl_2$ at 400 sec. Fura2 loaded parasites and Fura2 conditions were used. **G**, Same additions as in F but measuring fluorescence of GCaMP6. **H**, Response to the addition of 1 μM TG of the *iΔTgserca-sod2-gcamp6f* mutant (transfected with pCTH3-SOD2-GCaMP6f plasmid) previously grown in the presence (*pink trace*) or absence (*blue trace*) of ATc. The conditions for the fluorescence measurements are the same used in part G with intact parasites. The bar graph shows the ΔF measurements from three independent experiments. **I**, same as H but using 40 μM GPN. **J**, Same as H but using 100 μM Zaprinast. **K**, Same as H but using 1 μM Ionomycin. Data are presented as mean ± SD from 3 independent biological experiments. *p value*: unpaired two tailed t test performed in all comparisons.

F

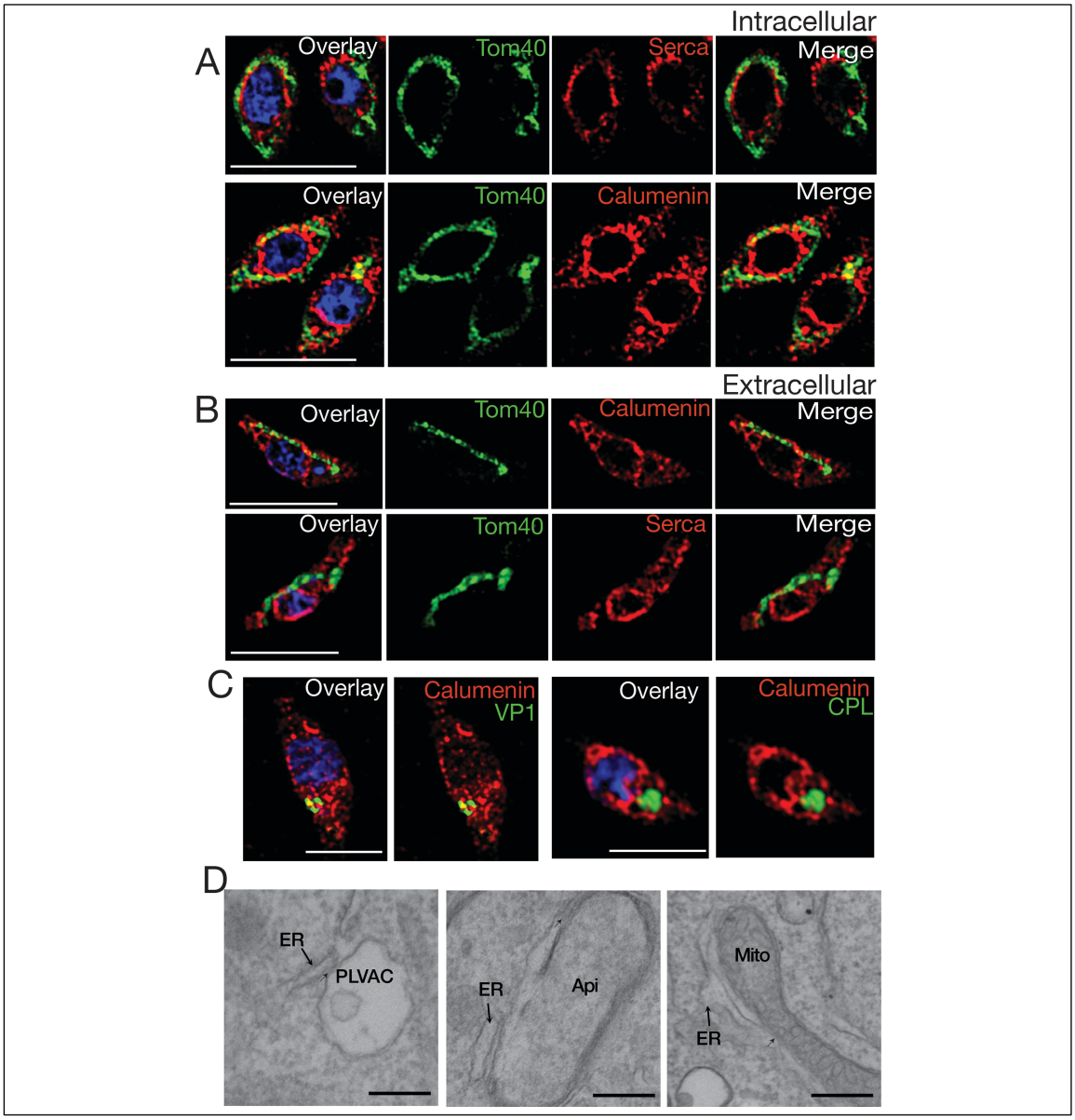

Figure 6: ER membrane contacts with the mitochondrion and the plant like vacuolar compartment (PLVAC). **A**, Super-resolution IFAs of intracellular parasites with the mitochondrion labeled with the αTom40 (green, 1:20,000) antibody and the ER labeled with the αTgcalumenin antibody (an ER calcium binding protein) (red, 1:1000) or the TgSERCA (red 1:1000). **B**, Immunofluorescence (IFA) of extracellular tachyzoites with the same antibodies used for part A. The mitochondrion and ER membranes interact in several regions. **C**, The PLVAC was localized with the αVP1 antibody (green, 1:200) or the αTgCPL antibody (green, 1:500). The ER membranes were labeled with the αTgERC antibody (red). The spots of contact between the ER and the PLVAC are yellow. Scale bars in A-C represent 5 μm. **D**, Transmission Electron Microscopy imaging of the contact sites formed between ER and PLVAC, ER and Apicoplast, ER and mitochondrial. Size bars are 100 nm.

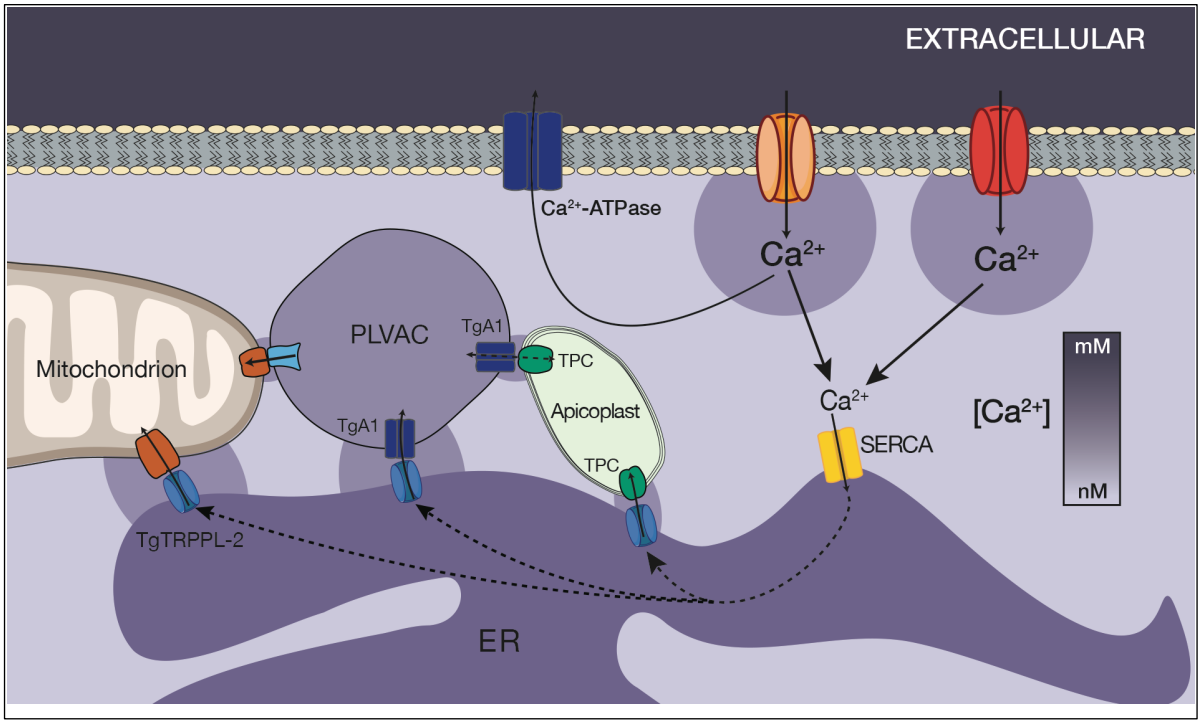

Figure 7: Model showing calcium entry through two different types of Ca^{2+} channels, uptake to the ER by SERCA and distribution to the other organelles via transfer from the ER to the mitochondria, PLVAC and apicoplast. In intracellular parasites, the mitochondria is in close contact with the ER which is constitutively leaking Ca^{2+} into the cytosol. The mitochondria take up Calcium from the ER through an unknown mechanism. VDAC could be involved in the transfer through the outer mitochondrial membrane (Mallo *et al.*, 2021). The PLVAC interacts with the ER and may also interact with the mitochondrion and the apicoplast. TgA1, a calcium ATPase previously characterized may be the pump involved in uptake (Luo *et al.*, 2001; Luo *et al.*, 2005). The mechanism of release is unknown. The TPC was shown to be involved in the formation of contacts between the ER and the apicoplast (Li *et al.*, 2021). Ca^{2+} could leak from the ER through the TgTRPPL-2 channel previously described (Marquez-Nogueras *et al.*, 2021).